CONSTRUCTION AND CHARACTERIZATION OF GENE REGULATORY NETWORKS IN YEAST

Daniel K. Jedrysiak

Thesis submitted to the Faculty of

Graduate and Postdoctoral Studies

In partial fulfillment of the requirements for the degree of

MSc Cellular and Molecular Medicine with Specialization in Bioinformatics

Department of Cellular and Molecular Medicine

Faculty of Medicine

University of Ottawa

ABSTRACT

CONSTRUCTION AND CHARACTERIZATION OF GENE REGULATORY NETWORKS IN YEAST

Daniel K. Jedrysiak

Department of Cellular and Molecular Medicine

MSc Cellular and Molecular Medicine with Specialization in Bioinformatics

Two major roadblocks in synthetic biology are the difficulties associated with the physical assembly of gene regulatory networks (GRNs) and the lack of characterized biological parts. In this work we aimed to address both of these issues. We developed a novel method for the assembly of GRNs called BrickMason assembly. We have shown that the method can assemble a 6 part network in a single day and provides significant advancements over traditional cloning methods. We used BrickMason to assemble GRNs that would allow us to compare natural yeast mechanisms of repression to the steric hindrance based mechanisms that are commonly used in synthetic GRNs in yeast. Our results show that the two mechansisms of repression are not equivalent. This finding opens possibilities for using a new class of repressor in a synthetic context in yeast.

ACKNOWLEDGMENTS

The completion of this thesis would not have been possible without the many people that helped me along the way. I would like to thank Dr. Mads Kaern for the mentorship, support, and guidance that he has provided me since my first summer as an undergrad student in his lab. It was an incredible learning experience not only academically, but outside of the lab as well. The unique opportunities that I was able to pursue as a member of his lab helped me to develop leadership and innovation skills that will stay with me for the rest of my life.

My thesis advisory committee, Dr. Ted Perkins and Dr. Adam Rudner, for providing a valuable outside perspective on my research.

Alex Power, who shared with me many of the discoveries related to the BrickMason protocols. If it wasn't Alex that developed a particular portion of the protocol, then it was still the result of one of our many insightful discussions. Without his contributions, none of this would have been possible.

Hilary Phenix for being one of the kindest and most genuine people I have ever encountered.

Mila Tepliakova for being my first teacher in the lab, who helped me numerous times, always with kindness and patience.

Nezar Abdennur and Daniel Charlebois for helping me with all of my modelling questions.

Sarah Voll for many great discussions.

And to my family and friends, especially my parents and my sister for their unwavering support and confidence, and whose sacrifices have allowed me to become the person that I am today.

Ottawa, September 2012

Daniel Jedrysiak

Contents

List of Figures

List of Tables

List of Abbreviations

Symbol	Description
2D	two dimensional
ATc	anhydrotetracycline
BE	β-Estradiol
BFP	blue fluorescent protein
CDS	coding DNA sequence
ChIP	chromatin immunoprecipitation
GFP	green fluorescent protein
GRF	gene regulatory function
GRN	gene regulatory network
iGEM	international genetically engineered machines competition
IPTG	isopropyl β-D-1-thiogalactopyranoside
NLS	nuclear localization signal
PCR	polymerase chain reaction
rtTA	reverse tetracycline transactivator
SB	synthetic biology
SC	synthetic complete
SLIC	sequence and ligation independent cloning
TBP	TATA binding protein
TF	transcription factor
tTA	tetracycline transactivator

Chapter 1

Introduction

1.1 Synthetic biology

Synthetic biology is an area of research at the interface of biology and engineering. There have been many attempts to engineer and design de novo life throughout the 20th century and as a result synthetic biology has roots in many fields [8]. Contemporary synthetic biology emerged at some point near the early 2000s. Dr. Tom Knight, a trained computer scientist, began taking molecular biology courses in the 1990s and by the year 2000 he had a fully operational biology lab located at the Artificial Intelligence Lab at MIT. Together with Dr. Drew Endy, a trained civil engineer, they organized the first synthetic biology conference in 2004. Inspired by the open source software model, advancements in synthetic biology have propagated through the undergraduate international genetically engineered machines (iGEM) competition and through the MIT Registry of Standard Biological Parts. iGEM teams or academic labs can obtain DNA fragments from the registry as long as they submit their new constructs back into the registry. This ensures collaboration and provides accessibility to the entire scientific community. Since its founding, international in-

terest in synthetic biology has steadily increased. Synthetic biology startups such as Amyris and LS9 are leveraging synthetic biology to bring real products into the market and the latest synthetic biology conference SB 5.0, held in June 2011, had over 700 participants from around the world.

1.1.1 Standardization and Abstraction

A central paradigm of synthetic biology is that of abstraction, a principle commonly used in engineering and computer science. For instance, a computer programmer does not need to program every aspect of a code. If a list needs to be sorted in the code, the programmer can use a sorting function created by someone else. If this function was well documented, the programmer only needs to know the function's valid input, and what output it will produce. This allows the programmer to create a complex code without having to rebuild every single component from scratch.

Biological systems are highly complex, and one method for managing this complexity is through abstraction [13]. A biological part in the context of synthetic biology is simply a sequence of DNA that has a particular function. Several biological parts can be combined, such as a promoter, coding DNA sequence (CDS), and terminator to produce a device and several devices can be combined to produce a system. This is known as an abstraction hierarchy and is shown in Figure 1.1. Each part, device, and system should have a standardized specification sheet that describes how the component functions across a valid range of input. For example, a properly characterized copper inducible promoter should specify the rate of transcriptional bursting initiated across a range of copper concentrations. The advantages of having standardized components is that they can function predictably off the shelf and can be incorporated in a plug and play manner. The researcher can model their system, choose the proper components from a library, assemble the parts, and have the system

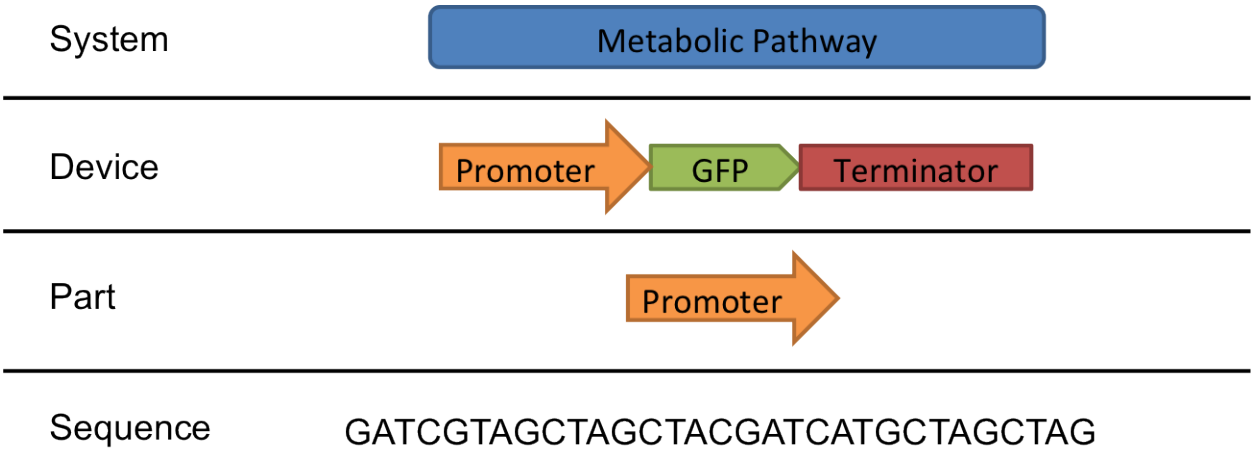

Figure 1.1 The abstraction hierarchy in synthetic biology adapted from [13]. Systems such as metabolic networks are created from devices, which in turn are created from parts. A part encapulates a DNA sequence, which is at the lowest level of abstraction.

work on the first try. Synthetic biology is still in its adolescence with respect to this vision. Efforts have been made to standardize components [9, 34], however this alone is a daunting task. Basic questions still need to be answered, such as: how should promoter strength be standardized, and in what context? These issues are further complicated by gene position effects. If something is characterized in one locus, does this mean we can predict its behaviour at another independent locus?

1.1.2 Progress in the field

In the year 2000, two seminal synthetic biology papers were published that laid the foundations for synthetic biology. These were the construction of the genetic toggle switch and the repressilator by Gardner et al. and Elowitz et al. respectively [12, 16]. These papers demonstrated the construction of the first synthetic dynamic gene regulatory networks and also showed that their function could be predicted by a computational model. Although both systems were constructed from very similar components, they had strikingly different behaviours. The toggle switch enabled non-genetic mem-

ory and the oscillator enabled periodic gene expression. Since this time, many new networks of increasing complexity have been created, including cascades [3], counters [15], oscillators [4], and memory loops [7] in both prokaryotic and eukaryotic systems. Advancement has slowed in recent years and although the number of gene regulatory networks created each year increases, their complexity does not [54]. Researchers agree that two major obstacles to progress in synthetic biology are the lack of standardized components and the difficulties associated with the physical assembly of these components [44].

The major goals of my thesis research are to contribute to the progress of synthetic biology by creating assembly methods to assemble gene networks more robustly and investigate new mechanisms of repression in synthetic eukaryotic gene regulatory networks.

1.2 Constructing gene regulatory networks

The discovery of the polymerase chain reaction (PCR) and restriction enzymes by Saiki et al. [58] and Smith et al. [62] respectively, has had a monumental impact on biological research. These techniques have been the driving forces behind recombinant DNA technologies by allowing us to copy and paste DNA sequences. The recent declining costs of de novo gene synthesis are allowing this technology to enter the molecular biologist's basic toolkit, functioning as the DNA equivalent of the word processor. It is still cost prohibitive to design genetic networks from scratch solely based on synthesis. At the time of this writing gene synthesis costs $0.38/bp and sequences up to 3 kb can be synthesized (Life Technologies). Larger sequences are more expensive and require custom pricing. The best approach for constructing gene regulatory networks on a large scale will come from the successful integration of di-

gestion/ligation and PCR with de novo gene synthesis. Therefore there is a demand for bridging the gap between synthesis and large scale pathway construction. Specifically, there is a need for technologies that can take smaller synthesized fragments and assemble them into larger constructs, bypassing the costs associated with synthesizing large fragments.

To be able to construct anything on a meaningful scale, it has to be possible to arrange parts in any order. These parts should also be easy to share with other researchers. To address these issues, Dr. Tom Knight proposed the BioBrick assembly standard 10 [38]. By adopting this standard, researchers would give up certain construction freedoms in exchange for ease of assembly and distribution of BioBrick parts.

A BioBrick is a segment of DNA that has a particular function, and under this assembly standard, the part must not contain EcoRI, XbaI, SpeI, or PstI restriction sites. BioBricks can be incorporated into plasmids that have the appropriate restriction sites and can be shared and propagated in *E. coli*. Two BioBrick parts can be assembled to create a new composite part. Part A is cut with EcoRI and SpeI, part B is cut with XbaI and PstI, and the destination plasmid is cut with EcoRI and PstI. Ideally, we would expect the EcoRI overhang in part A to bind to the EcoRI overhang in the destination plasmid, the PstI overhang in part B to bind to the PstI overhang in the destination plasmid, and SpeI to bind with XbaI and form a mixed site (BioBrick scar) that is undigestable by any of the standard BioBrick enzymes. The resulting part AB is now located in a plasmid, prefixed by EcoRI and XbaI, and suffixed by SpeI and PstI. In this sense the assembly is idempotent and any composite BioBrick part can be used as a BioBrick in subsequent assemblies. A detailed overview of this process is described in the literature [38]. Along with the creation of the BioBrick assembly standard 10, the BioBrick registry of standard biological parts was created

at MIT. Researchers can obtain BioBricks parts from the registry free of charge, and in exchange are expected to donate their new BioBrick parts back to the registry.

The BioBrick assembly standard 10 has accelerated research in many labs across the world (any successful iGEM project can be taken as evidence), and increased collaboration internationally. However the assembly standard suffers from several drawbacks. Sometimes it is impossible or impractical to remove all of the illegal restriction enzymes from a sequence. Such parts can never be assembled within the BioBrick framework. The creation of a mixed site between parts may be intolerable, for example when precisely inserting repressor binding sites into proximal promoters. The assembly itself is very slow. Parts can be assembled in parallel, however, each assembly of two parts still takes 3 days to complete since the parts need to be transformed into *E. coli*. The actual assembly can be difficult to achieve, especially when larger sequences are used. The destination plasmid may self ligate, resulting in an intolerable number of false positive colonies on the transformation plate.

There are several assembly protocols that have been proposed as alternatives to the BioBrick assembly standard 10. The in-fusion BioBrick assembly protocol uses a proprietary Clonetech polymerase [70] that relies on nick and gap repair by transformation into *E. coli*. The authors show that up to 3 parts can be assembled simultaneously, although the efficiency is only 37%. The assembly of two parts has a higher efficiency, between 61.8% and 84.8% depending on the length of the overhangs used [60]. The increased number of possible components that can be assembled and avoiding the use of restriction enzymes make this method more attractive then BioBrick assembly standard 10. Problems with longer sequences are anticipated with inserting the final construct into a vector.

Other methods such as MoClo are more amenable to parallelization [67]. The authors show that this method is capable of assembling a 33 kilobase fragment from

44 parts in 3 cloning steps. The method relies on the use of two type IIs restriction enzymes, Bpil and BsaI. The restriction enzymes recognize a standard sequence, but are able to cut several base pairs away.

Because the cleavage occurs adjacently to the restriction site, the single pair of enzymes can be used to create a large number of custom overhangs. Many byproducts of digestion/ligation can be eliminated by choosing non-palindromic overhangs which prevent the autoligation of DNA fragments. The method is highly parallelized and multiple fragments can be assembled in a single step. The drawbacks of this approach are that parts are not interchangeable due to custom overhangs and scars are introduced between parts. This means that new parts have to be generated every time a new system is to be constructed.

A better approach would be to eliminate restriction enzymes and rely on PCR and homologous recombination to assemble DNA fragments. Sequence and ligation-independent cloning (SLIC) is a method for performing in-vitro homologous recombination. However, a 10 piece assembly only had a 17% success rate [42]. An alternative approach is to take advantage of natural homologous recombination machinery by performing the assembly in vivo. DNA assembler is a method for transforming individual DNA fragments into yeast cells, and having the cells assemble the final construct by recombination [59]. A similar assembly has been performed with oligonucleotides. This allows overlaps between consecutive fragments to be as short as 20 bp, however double stranded PCR products cannot be used in this assembly [18]. Assembly methods that rely on in vivo recombination have their own problems including the difficulty of transforming all the fragments into a single cell, and the non specific integration of DNA fragments into the genome. Yeast spheroplasts can be prepared to increase the permeability of DNA, however this is a long process and cells take longer to grow on transformation plates [39]. Despite these drawbacks, in vivo re-

combination has also proven to be highly effective, and even allows the manipulation of entire genomes. This was the method used by Gibson et al. to assemble the first synthetic genome [19].

Perhaps the most popular assembly method used in synthetic biology is the Gibson isothermal approach [20]. DNA fragments are amplified by PCR, adding 40 bp of homology to neighbouring pieces. The DNA fragments are pooled into a single reaction at 50 °C containing T5 exonuclease, Phusion polymerase, and Taq ligase. The T5 exonuclease chews back the 5' ends of double stranded DNA. The exposed overhangs can bind to homologous fragments, gaps are filled by the Phusion polymerase, and nicks are ligated by the Taq ligase. A drawback of this method is that it is possible for the T5 exonuclease to digest small fragments to completion, making it hard to assemble fragments in the 100 bp range. For example, when assembling a 100 bp fragment, 40 bp are used for homology on either end of the fragment, this only leaves 20 bp of double stranded DNA. This 20 bp of double stranded DNA could be digested to completion by an overactive exonuclease, making the fragment unable to participate in the assembly.

The ideal assembly standard must allow the researcher to assemble DNA parts in a predetermined order, with no scars or restrictions on usable sequences. The method must also allow parallel assembly and must function at any scale [10]. Currently there is no technique that can cover all these cases. We chose to focus on developing an assembly method that can use fragments in the 100 bp - 3 kb range and bridges the gap between gene synthesis and large network assembly.

1.3 Characterizing gene regulatory networks

Similarly to the physical construction of GRNs, the characterization of GRNs is another important component of synthetic biology. The characterization of a GRN enables the construction of a computational model for that GRN and allows the researcher to make modifications to the network in both a rational and predictable manner. The first synthetic GRNs were constructed using drug-inducible components. A model could be constructed by varying the activity of each component using a drug and measuring the effect on the reporter, a fluorescent protein [16]. Advancements in fluorescent protein technology increased the number of points in a network that could be measured simultaneously [21]. This led to the development of the gold standard in network characterization, the gene regulatory function (GRF) [56]. The GRF is the quantitive relationship between transcription factor concentration and the rate of protein production from the downstream promoter [56]. It can obtained by measuring a fluorescent reporter expressed from the downstream gene across varying levels of a fluorescently tagged transcription factor. GRFs have been measured in eukaryotes using fluorescent microscopy [35]. The advantage of fluorescent microscopy is that data can be collected on the localization of the transcription factors providing a clearer picture of the fraction of transcription factor that is transported into the nucleus. The disadvantage is that this is not a high throughput method. Slides must be prepared by hand and exposure times as long as 5 minutes are needed to visualize the fluorescently tagged transcription factors. We chose to focus on the development of a flow cytometry-based method for the measurement of GRFs that would allow for high throughput data collection.

1.4 Mechanisms of activation

Inducible promoters are essential components of natural GRNs. They enable cells to respond to changing environments. In yeast, common inducible promoters include the copper [45], phosphate [35], and galactose promoters [53]. The *GAL1* promoter is a divergent promoter that shares an upstream activation sequence with *GAL10*. It is known to be one of the strongest promoters in yeast [46]. Gal4p is the main activator of the *GAL* genes. In the absence of galactose, Gal4p is inhibited by Gal80p. In the presence of galactose, Gal3 is activated and relieves the repression of Gal4p by Gal80p. The *GAL1* promoter drives the expression of genes that allow the cell to metabolize galactose for use as a carbon source when glucose is unavailable. The *GAL1* promoter has a very switch-like response to glucose due to a Gal1p positive feedback loop mediated by Gal4p [29]. In many cases, it is desirable for inducible promoters to exhibit a graded response to the inducer rather than an all-or-none response. Inducers may also have physiological effects on the cell, such as galactose, which causes a decrease in growth rate [26]. Heterologous induction systems can overcome these problems since the cells are unaffected by the inducer. An example of such a system is the Gal4-ER-VP16 (GEV) activator. This is a fusion protein containing the Gal4p binding domain, the human estrogen receptor, and the VP16 activation domain [43]. The Gal4p binding domain binds DNA as a dimer [27], and the fusion protein can only dimerize in the presence of β-Estradiol due to the human estrogen receptor protein domain. The *GAL4* can be replaced with the GEV construct and *GAL1* promoters will become responsive to β-Estradiol. Cells can be grown in glucose without reducing their growth rate and the *GAL1* promoter will exhibit a graded response to β-Estradiol since there are no feedback loops in this synthetic network [29]. Due to these advantages, the GEV activator was used in this

research.

1.5 Mechanisms of repression

It is important to understand the mechanisms behind biological processes in order to create mathematical models that describe them. The repression of a gene at the transcriptional level is one of the most basic processes in a gene regulatory network. Prokaryotes and eukaryotes have inherently different mechanisms of repression [64], however it is unclear how this affects their behaviours. Many studies have used prokaryotic mechanisms of repression in eukaryotic organisms to make conclusions about eukaryotic transcription [3, 11, 47, 48]. It is therefore important to perform a side by side comparison of the two mechanisms and characterize their differences.

LexA is a repressor protein in E. coli that represses genes involved in the S.O.S response [14]. LexA was the first bacterial repressor shown to function in yeast [5]. This was a significant contribution to the construction of GRNs, since for the first time it was shown that it is possible for a heterologous prokaryotic repressor to function in eukaryotic cells. This finding meant that the LexA repressor protein was correctly being synthesized, dimerizing, crossing the nuclear membrane, and finding its operator site in the yeast genome. Repression was achieved when the LexA operator sites were inserted between the upstream activation sequence (UAS) and the transcription start site of the endogenous Gal1 promoter. The authors hypothesized that the mechanism of repression by LexA was likely interfering with the proper assembly of transcriptional machinery.

The heterologous *E. coli* repressor proteins LacI and TetR were subsequently shown to function in mammalian cells [23,30]. This was also a significant contribution since LacI and TetR dimerization could be controlled by IPTG and Tetracycline

respectively, allowing for the creation of inducible gene regulatory systems. Until this point, these repressor proteins were being used to repress activated genes. A problem with this approach was that the repressor needed to be very strong in order to prevent any leaky expression. Since the promoter would always be in the "on" state, any inefficiencies in the chain of events from repressor synthesis to DNA binding could lead to a burst of expression.

Researchers continued to search for expression systems that would allow for tighter control of gene expression. It was discovered that chimeric transactivators could be created by fusing an activation domain, such as Gal4p in *S. cerevisiae*, to a DNA binding domain such as LexA [6]. When the transactivator bound near a minimal promoter, it could drive protein expression. When the DNA binding domain was switched for a DNA binding domain of an inducible protein, the level of activation could be controlled [40]. Rather then repressing a gene whose promoter was always in the"on" state, much tighter expression could be achieved by directly controlling the activation of that promoter. This system was improved by swapping the LacI with the TetR repressor [23] and became known at the TetR transactivator system (tTA). Due to the tight regulation achieved by this system it was widely used and became the most popular choice for controlling protein expression in eukaryotic cells. A reverse TetR transactivator (rtTA) was created that bound DNA in the presence of tetracycline or other analogous molecules [24]. Interest in repression began to resurface because the reverse TetR DNA binding domain could be used to gain even tighter control over gene expression. By fusing an activation domain to the reverse TetR and a repression domain to TetR, gene expression could be both activated in the presence of Tetracycline analogue and repressed in its absence [1]. The repression domain used in this context was SSN6 and this system of repression represents the first attempt to emulate native yeast repression mechanisms in a synthetic system.

When the first synthetic biology gene networks began appearing in yeast, the mechanism of repression chosen in these networks was steric hindrance [17]. This repression mechanism was probably chosen due to the similarity to mechanisms of repression in *E. coli* and the lack of understanding surrounding native yeast repression. The steric hindrance repression mechanisms were characterized [47], and subsequently became standard components for use in yeast synthetic biology. As a result, there has been a significant amount of research about noise [47], development of drug resistance [2], and linearity [48] in systems that use steric hindrance based repression. However it is unclear that these systems behave like natural eukaryotic mechanisms of repression.

Ratna et al. were the first to revisit the use of eukaryotic repression mechanisms in yeast in a synthetic context [55]. They examined the effect of Cyc8-TetR and Sir3-TetR fusions binding at various positions around the Gal1 promoter. They did not, however, examine the effect of repression when these repressors bound at the natural Mig1 binding sites within the Gal1 promoter. Interestingly they found that both repressors created a repression gradient, something that is not observed through steric hindrance repression mechanisms. However, there still has not been a side by side comparison of steric hindrance based repression to natural yeast repression mechanisms.

In this work, I focus on repression by Cyc8, which is part of one of the best studied repressor complexes in yeast. Cyc8 was first identified in yeast as a repressor of cytochrome C expression [57] and it was subsequently discovered that it forms a complex with Tup1 [68]. The Cyc8-Tup1 complex was found to repress a diverse set of genes, and was identified as a general repressor of transcription in yeast [33]. Further analysis of the Cyc8-Tup1 repressor complex revealed that Tup1 played a major role in repression independent of Cyc8 and the ability of Cyc8 to repress in

Δ*tup1* strains was inhibited. Therefore, Cyc8 was thought to act as an adapter between the DNA binding protein such as Mig1 and Crt1, and the repressor Tup1. This type of mechanism would allow for a high degree of specificity and diversity of repression. In fact, the Cyc8-Tup1 repressor complex is responsible for the repression of 3% of yeast genes [63].

The Cyc8-Tup1 complex has been shown to be involved in a diverse set of processes related to transcription from activation [51] to interacting with the mediator complex [50]. Recently Wong et al. [69] have published the most comprehensive analysis on the mechanics of Cyc8-Tup1 repression performed to date. All the previous studies rely on highly synthetic systems, and deletions that significantly alter growth rate. Also many of these processes cannot be disabled with a single deletion. Wong et al. use the anchor away method and follow occupancy at the promoter using ChIP. This method removes a protein of interest from the nucleus of a cell by conditionally tethering it to a ribosomal protein that flows out of the nucleus. Their analysis is likely to reveal the mechanics behind Cyc8 repression because they are analyzing the repression in the most natural state. Wong et al. demonstrate that when Cyc8-Tup1 is removed from the nucleus, Swi/Snf, SAGA, and the mediator complex are rapidly recruited to the promoter. When Cyc8-Tup1 is reintroduced to the nucleus (through induction by galactose), Swi/Snf, SAGA, and the mediator complex are evicted from the promoter. It is important to note that this happens before the formation of any repressive chromatin structure. The authors hypothesize that the Cyc8-Tup1 complex does not evict or inhibit the binding of the activator. Instead, the Cyc8-Tup1 complex binds and blocks the domain of the activator protein that is responsible for coactivator recruitment. A repressive chromatin structure is then formed through the yeast's natural tendency to deacetylate nucleosomes [69].

The steric hindrance repression mechanisms repress transcription by interfering

with the binding of TBP, while Cyc8 represses transcription at multiple levels and involves a diverse set of transcriptional machinery. This thesis will focus on characterizing both mechanisms of repression with the aim of determining if mechanistic differences have significant effects on behaviour.

1.6 Hypothesis

We hypothesize that steric hindrance and natural yeast repression mechanisms are not equivalent and can have significant impact on gene expression dynamics.

1.7 Specific aims

The main focus of this work is to contribute to the advancement of synthetic biology in yeast. This will be accomplished by focusing on two major obstacles identified in the literature, the difficulty with physically assembling GRNs and the lack of characterized components. We aim to develop a new method of assembly that targets constructs in the 100bp-3kb range for the creation of final constructs in the 10 bp range. We also aim to perform a side by side characterization of steric hindrance and natural yeast repression mechanisms. Natural yeast repression mechanisms are rarely used in synthetic GRNs in yeast. We hope that our characterization will provide researchers with a new component for use in synthetic networks.

1. Develop a method for the rapid assembly of GRNs in yeast.

2. Benchmark the assembly method by determining the error rate.

3. Design and construct a network for the measurement of GRFs by flow cytometry.

4. Construct two promoters and their corresponding repressors that are representative of steric hindrance and natural yeast repression.

5. Perform dose response experiments to record GRFs for both repression mechanisms.

Chapter 2

Methods

2.0.1 Genomic extraction

A single yeast colony was inoculated into 10 mL YPD and grown overnight. The sample was spun down to 3000g for 5 minutes. The pellet was resuspended in 500 μL of autoclaved ddH_2O, and transferred to a micro-centrifuge tube. The sample was spun down at 5000g for 30 seconds and the supernatant was discarded. The cells were resuspended in 200 μL breaking buffer, 300 mg of acid-washed glass beads, and 200 μL of phenol:chloroform:isoamyl alcohol (25:24:1). The sample was vortexed at maximum speed for 3 minutes, then 200 μL of TE buffer was added and the sample was vortexted for 10 seconds. The sample was spun down at 13000g for 5 minutes and the supernatant was discarded with a pipette. The pellet was resuspended in 430 μL of TE buffer, 1 μL of 32μg/μL of RNaseA was added and the sample was incubated for 5 minutes at 37 °C. 10 μL of 4 M ammonium acetate and 1 mL of 100 % ethanol were added, and the sample was mixed by inversion. The sample was spun down at 13000 g for 3 minutes, the supernatant was discarded, the sample was inverted and air-dried for 30 minutes. The pellet was resuspended in 100 μL TE buffer. **Media: Breaking buffer**. 2% (v/V) Triton X-100, 1% (w/v) SDS, 100 mM NaCl, 10 mM

Figure 2.1 Design of standard forward and reverse BioBrick primers.

Tris-HCl pH 8.0, 1 mM EDTA pH 8.0. **TE buffer**. 10 mM Tris-HCl pH 8.0.

2.0.2 Primer design

BioBrick primers were designed as shown in figure 2.1. The forward primer contained EcoRI and XbaI restriction sites and the reverse primer contained PstI and SpeI restriction sites. Between 17-20 bp of homology to the part was chosen to maximize similarity in melting temperature between primer. In general, we aimed for a melting temperature of 60 °C for the entire primer.

BrickMason v2.0 primers were designed to enable maximum reusability. The reverse primer for a part was designed to be reused in any assembly and was homologous to the last 25 bp of a part. The forward primer was specific to a particular assembly and contained 25 bp homology to the preceding part followed by 25 bp of homology to the current part. We aimed to achieve melting temperatures of 60 °C for the entire forward primer.

2.0.3 Yeast transformations

The Gietz transformation protocol [22] was adapted with small modifications. All transformations were genomically integrated and the entire available DNA sample

was used for transformation (200 - 1000 ng). For drug selection, after heatschock cells were allowed to recover overnight in YPD before plating directly onto drug containing plates.

2.0.4 Plate based collection of flow cytometry data

The Cyan ADP 9 flow cytometer (Beckman Coulter) was used to capture flow cytometry data. For quantifying BFP expression, a 405nm laser was used for excitation with a 530/40nm filter. For quantifying GFP expressison, a 488 nm laser was used for excitation with a 530/40nm filter. Before measurement by flow cytometry, samples grown in YPD media were diluted 1/10 in water and samples grown in synthetic complete (SC) media were diluted 1/2. 200 uL of the diluted samples used for analysis. A 15 second sip time, a 1.2 second up time, and a 10 second pause time between rows were set for sample acquisition. Data for the whole plate was collected in a single .fcs data file. Intellicyt Hyperview Analysis Version 3.3.3665.28886 software was used to manually split the data into separate well files.

2.0.5 Analysis of flow cytometry data

Flow cytometry data was analyzed using Kaluza Flow Cytometry Analysis v1.2 software. A manual gate was used to select the most dense cellular population on the forward scatter vs side scatter plot of the wild type sample and was identically applied to all other samples.

2.0.6 BrickMason v 1.0

Parts A and B are PCR amplified in a 50 μL reaction as shown in table 2.1. For each part the forward primer added an XbaI restriction site and the reverse primer added

an SpeI restriction site, therefore standard BioBrick primers can be used for this assembly. Parts used in this assembly cannot contain XbaI or SpeI restriction sites within their sequence. Both parts were run on a gel, extracted, and column purified. Part A was digested with SpeI and part B was digested with XbaI as shown in table 2.2, the reaction was run for 30 minutes at 37 °C. 1 μL of antarctic phosphatase and 3 μL of antarctic phosphatase buffer were added to part B and the reaction proceeded for an additional 20 minutes at 37 °C. The samples were column purified and eluted in 30 μL. 2 μL of each sample was used for determining DNA concentration using the NanoDrop 3300 fluorospectrometer. Parts A and B were ligated, as shown in table 2.3, the ligation was run for 5 minutes at 16 °C and then denatured for 20 minutes at 80 °C. The reagents in table 2.4 were added to this reaction in order to digest away any homodimers, the digest was run for 20 minutes at 37 °C and denatured for 20 minutes at 80 °C. The reaction was subsequently used in a PCR reaction with the forward primer for part A and the reverse primer for part B as shown in table 2.5. The PCR reaction was run on a gel, and the correct dimer was extracted, column purified, and eluted in 30 μL. 2 μL was used for determining DNA concentration and the reagents in table 2.6 were added to digest the ends of the dimer. This digest was run for 40 minutes at 37 °C and was denatured for 20 minutes at 80 °C. This dimer can now be combined with other overlapping dimers in a final PCR reaction as shown in table 2.7. The whole BrickMason v1.0 assembly protocol is summarized in figure 2.2.

2.0.7 BrickMason v 2.0

An overview of the BrickMason is shown in figure 2.3. For the assembly of a dimer, parts A and B were each PCR amplified with their corresponding BrickMason v2.0 primers. The forward primer for part B introduces 20 bp of homology to the 5' end

Table 2.1 The first PCR reaction in the BrickMason v1.0 protocol

Reagent	**Amount μL**
5x HF reaction buffer	10
10 mM each dNTP mix	1
FP	0.25
RP	0.25
Template DNA	20 ng
Phusion polymerase	1
H_2O	rest
Total:	**50**

Table 2.2 The first digestion reaction in the BrickMason v1.0 protocol.

Reagent	**Amount μL**
NEB Buffer 2	3
BSA (10x)	3
SpeI or XbaI	0.5
DNA	22.5
H_2O	1
Total:	**30**

Table 2.3 Ligation of two monomers in the BrickMason v1.0 protocol

Reagent	**Amount μL**
NEB Buffer 2	2
10 mM ATP	2
T4 DNA ligase	0.5
Part A	100 ng
Part B	100 ng
H_2O	rest
Total:	**20**

Table 2.4 The second digestion reaction in the BrickMason v1.0 protocol, for the removal of homodimers. These reagents are added directly into the denatured ligation reaction

Reagent	**Amount μL**
NEB Buffer 2 (10x)	0.5
BSA (10x)	2.5
XbaI	0.5
SpeI	0.5
H_2O	1
Total:	**5**

Table 2.5 Second PCR reaction in the BrickMason v1.0 protocol, for amplification of dimers.

Reagent	**Amount μL**
5x HF reaction buffer	10
10 mM each dNTP mix	1
FP	0.25
RP	0.25
Template DNA	4
Phusion polymerase	1
H_2O	33.5
Total:	**50**

Table 2.6 Digestion of the amplified dimer in the BrickMason v1.0 protocol

Reagent	**Amount μL**
NEB Buffer 2	4
BSA (10x)	4
XbaI	1
SpeI	1
H_2O	5
Total:	**15**

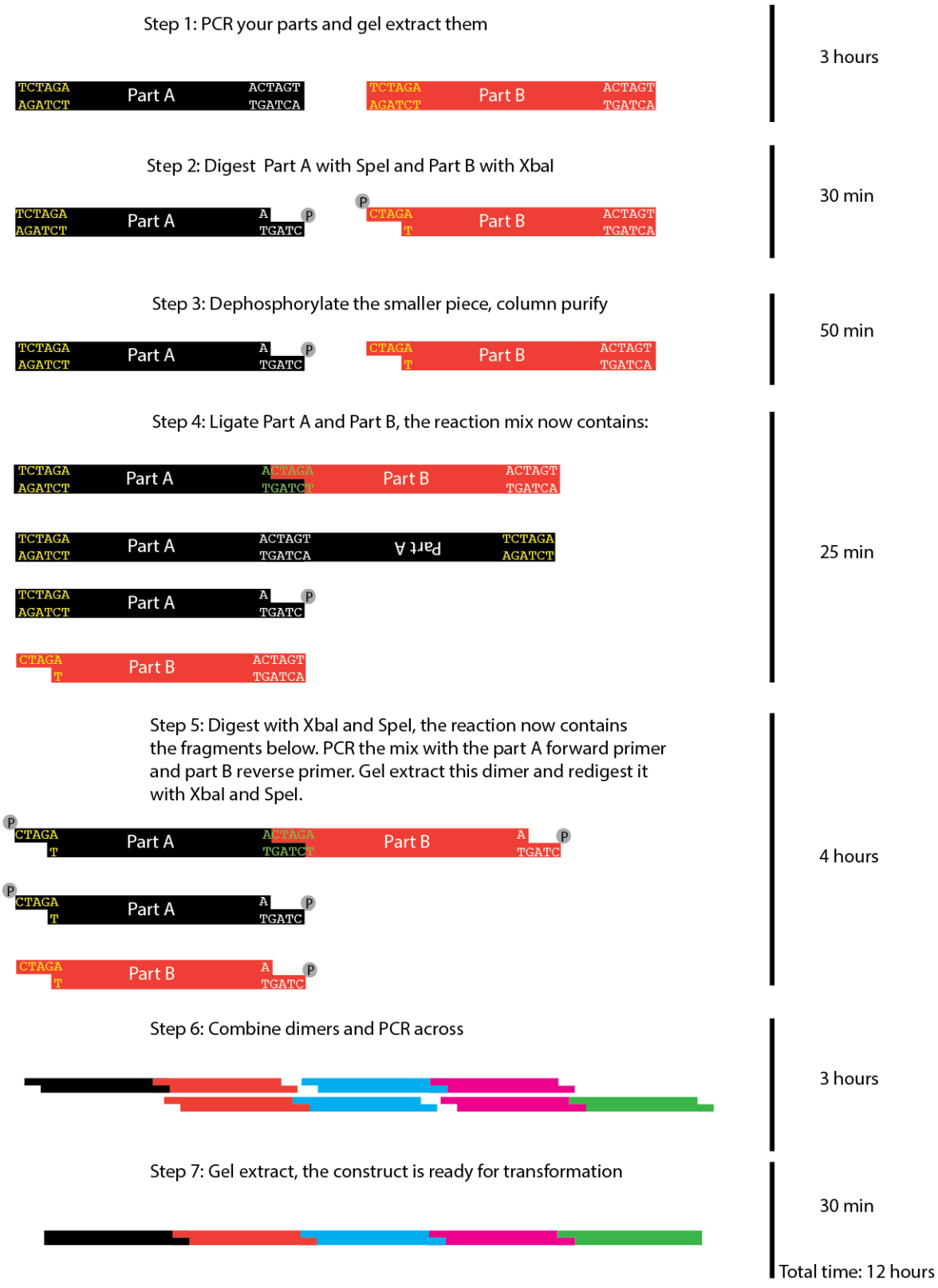

Figure 2.2 Overview of the BrickMason v1.0 protocol.

Table 2.7 Final PCR in the BrickMason v1.0 protocol for the assembly of a multimer from dimers.

Reagent	**Amount μL**
5x HF reaction buffer	10
10 mM each dNTP mix	1
FP	0.25
RP	0.25
Phusion polymerase	1
DNA (each piece)	25 ng
H_2O	rest
Total:	**50**

of part A. A 2 μL aliquot of each part is run on a gel for confirmation, the remaining sample is column purified. A subsequent PCR reaction is performed, creating an AB dimer as shown in table 2.8. In a similar reaction to the final PCR step in the BrickMason v1.0 protocol, the dimer can be combined with other overlapping dimers to obtain the final construct.

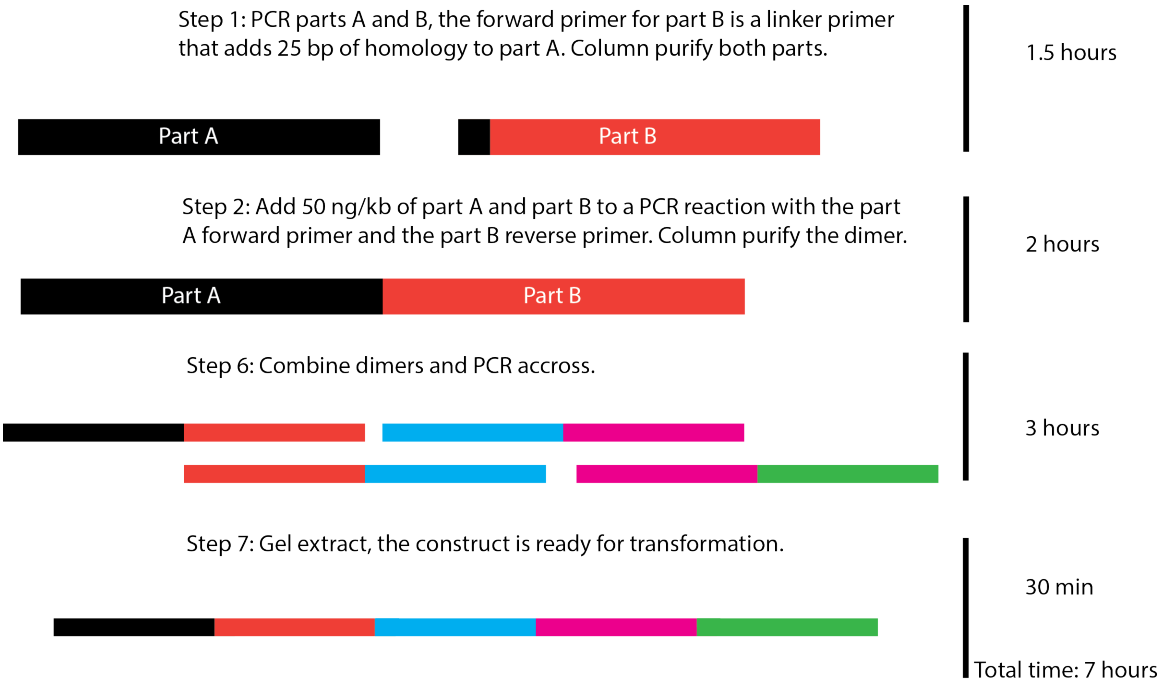

Figure 2.3 Overview of the BrickMason v2.0 protocol.

Table 2.8 PCR reaction joining two fragments in the BrickMason v2.0 protocol.

Reagent	**Amount μL**
5x HF reaction buffer	10
10 mM each dNTP mix	1
FP for part A	0.25
RP for part B	0.25
Part A DNA	50 ng/kb
Part B DNA	50 ng/kb
Phusion polymerase	1
H_2O	rest
Total:	**50**

Chapter 3

Results

3.1 BrickMason v1.0 protocol

3.1.1 YBA3 construction

The YBA3 GRN shown in figure 3.1 was constructed using the BrickMason v1.0 protocol from the 6 monomers listed in table 3.1. YBA3 consists of the KanMx selection marker (provides resistance to the drug G418) and the constitutive TDH3 promoter driving a Ura3-GFP fusion protein. These components are flanked by the Ade2 up and Ade2 down constructs, which have homology to the *ADE2* locus in yeast. When YBA3 is successfully inserted into the *ADE2* locus, the cells will have a red phenotype due to disruption of the native *ADE2* gene. Therefore, cells that have successfully integrated YBA3 in the correct locus should appear red, be resistant to G418, grow on uracil deficient media, and express GFP. The function of each component of YBA3 can be easily assessed by screening, making this construct well suited for benchmarking the BrickMason assembly method. Each monomer was amplified by PCR using standard BioBrick primers. The forward primer added EcoRI, NotI, and XbaI restriction sites and the reverse primer added XbaI, NotI, and PstI restriction sites.

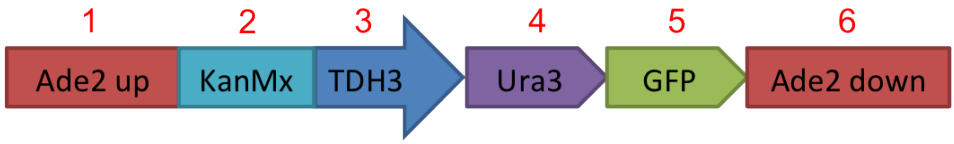

Figure 3.1 Diagram of the YBA3 construct. Ade2 up and Ade2 down are 200 bp regions that have homology to the *ADE2* locus in yeast. KanMX is a selection marker that provides resistance to the drug G418. TDH3 is a constitutive native yeast promoter and is driving the expression of a Ura3-GFP fusion protein. The Ura3 gene allows yeast to surive on -Ura media.

Each monomer was run on a gel, extracted, and purified as shown in figure 3.2. The monomers were used to assemble the dimers listed in table 3.1 as described in the BioMason v1.0 protocol. The dimers were run on a gel shown in figure 3.3. Although multiple bands are present in each lane on the gel, the darkest band corresponds to the correct dimer. The correct dimer was cut out from each lane and gel purified. The dimers were digested with SpeI and XbaI to make the ends of each DNA fragment compatible for the final assembly. The 5 overlapping dimers were combined in a final PCR reaction to generate the YBA3 construct shown in figure 3.4. YBA3 was cut out of the gel and purified. The whole purified sample was transformed into BY4742 using a standard yeast transformation and plated on YPD + 200 mg/mL G418.

3.1.2 Screening YBA3 yeast colonies by color

The YBA3 construct contains the Ade2 up and Ade2 down regions, which are 200bp segments that target the integration of the construct at the *ADE2* locus [25]. The construct also contains a KanMX marker and a GFP tagged Ura3 marker which are both constitutively expressed. Since the YBA3 transformant cells were plated onto media that did not have supplementary adenine, they must rely on their native adenine pathway for its synthesis. A disruption in the *ADE2* gene is known to produce

Table 3.1 The number, name, primers, and size of each part used in the YBA3 construction. Parts 1-6 are monomers and the rest are dimers.

Number	**Part**	**FP**	**RP**	**Size (bp)**
1	Ade2 up	P34	P35	234
2	KanMX	K54	K61	1424
3	TDH3	M28	M29	725
4	Ura3	J65	J66	801
5	GFP	K59	K60	714
6	Ade2 down	P36	R57	288
12	Ade2 up - KanMX	P34	K61	1658
23	KanMX - TDH3	K54	M29	2149
34	TDH3 - Ura3	M28	J66	1526
45	Ura3 - GFP	J65	K60	1515
56	GFP - Ade2 down	K59	R57	1002

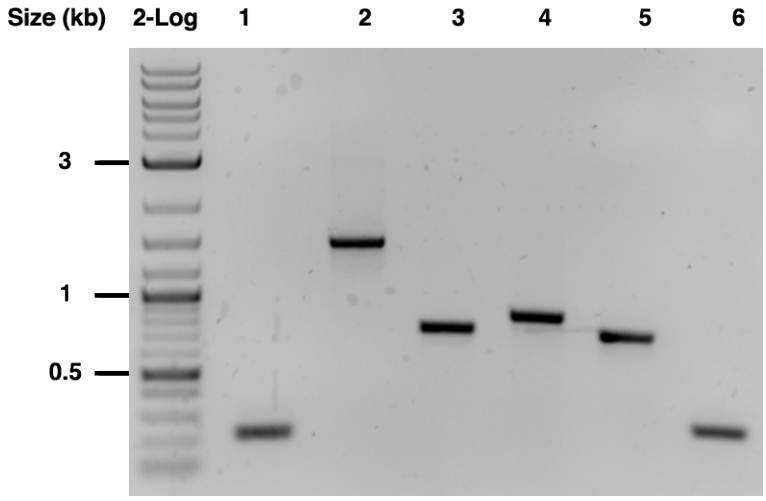

Figure 3.2 Monomer parts 1-6 from the YBA3 assembly. Each monomer was obtained by PCR amplification of template DNA with standard BioBrick primers and 3 μL was run on a gel for confirmation. The size and part name of each monomer are listed in table 3.1. The monomers were gel extracted and used for making dimers in the next step of the BrickMason v1.0 protocol.

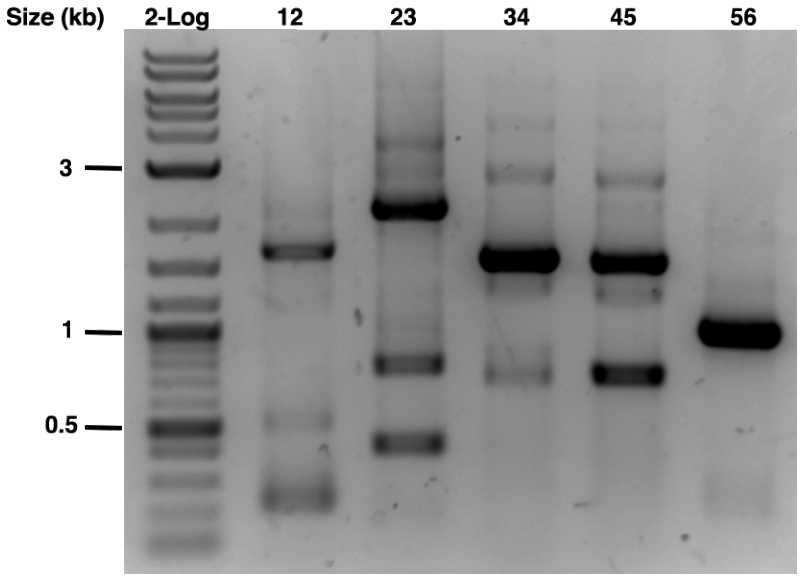

Figure 3.3 Dimer parts 12-56 from the YBA3 assembly. Each dimer was obtained by assembling two monomers through the BrickMason v1.0 protocol. The darkest band in each lane corresponds to the correct fragment. The size and name of each dimer are listed in table 3.1. The dimers were gel extracted and used in the final PCR step.

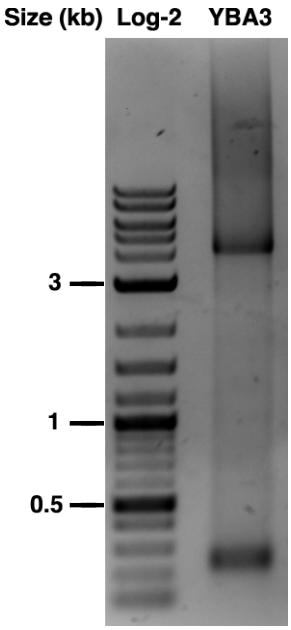

Figure 3.4 The final YBA3 construct, was assembled from pooling the dimers and performing a PCR reaction as described in the BrickMason v1.0 protocol. The expected size of YBA3 is 4216 bp and a band of this size is clearly visible. The band was cut out, gel purified, and used in the subsequent transformation.

Figure 3.5 Red and white BY4742 colonies following transformation of the YBA3 construct. Cells are grown on YPD plate supplemented with 200mg/L G418. A red colony indicates a successful disruption of the *ADE2* gene. 16 red colonies from this transformation plate were chosen for analysis.

a red phenotype due to the accumulation of red pigmented metabolic precursors in the vacuole [66]. Red colonies on the YBA3 transformation plate indicate that the YBA3 construct has likely been integrated into the correct locus, whereas white colonies indicate a construct integrated at an incorrect locus. Red colonies that grow on G418 supplemented media, grow on uracil deficient media, and express GFP are likely to contain the assembled construct integrated at the correct locus. Figure 3.5 shows a close up picture of the YBA3 transformation plate, red and white colonies are easy to distinguish. 16 colonies from this plate were subsequently streaked out onto yeast synthetic dropout media without uracil. All 16 colonies were able to grow on this media and the wild type BY4742 strain was not as shown in figure 3.6. This indicates that all 16 colonies are correctly expressing the Ura3p portion of the Ura3-GFP fusion protein, they are correctly expressing KanMX, and the whole YBA3 construct is integrated at the *ADE2* locus.

3.1.3 Screening YBA3 yeast colonies by flow cytometry

In order to determine if the colonies were expressing GFP, cells were analyzed by flow cytometry. Overnight cultures of the 16 YBA3 strains and the wild type BY4742

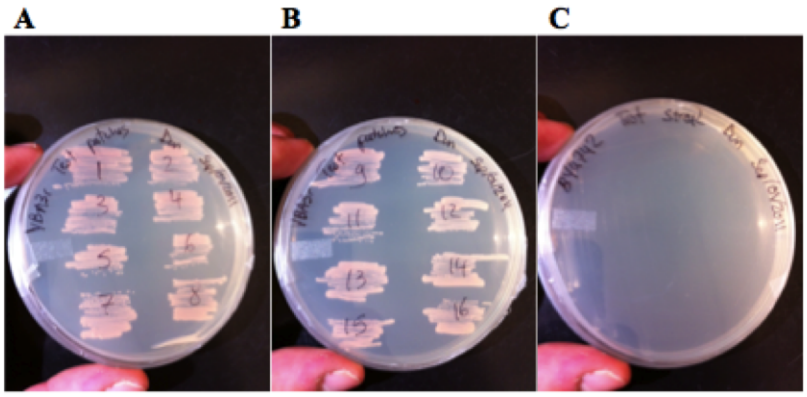

Figure 3.6 16 red colonies from the transformation plate were streaked out in patches onto yeast synthetic dropout media without uracil. (**A**) colonies 1-8, (**B**) colonies 9-16, (**C**) wild type BY4742. All the transformed colonies were able to grow, indicating the correct expression of the *URA3* gene.

strain were analyzed for GFP expression. Figure 3.7 shows that only 6 out of 16 colonies expressed GFP, corresponding to a 38% success rate. The cells that did express GFP all had very similar expression suggesting that the constructs did not accumulate many mutations through multiple round of PCR.

3.1.4 Sequencing YBA3 colonies

The 16 YBA3 colonies were analyzed by sequencing. A genomic extraction was performed on each sample and the entire YBA3 construct was PCR amplified. 9 sequencing primers were used, that bound roughy 500 bp apart, shown in table 3.2. Sanger sequencing was performed by the Sick Kids hospital in Toronto.

A custom MatLab script based on the Bioinformatics toolkit was used to analyze the sequencing. A reference sequence was built based on what we expected the YBA3 sequence to be. The first and last 20 bp of each sequencing read were discarded from the analysis. For each primer, the associated sequencing results were aligned to the reference sequence using a local alignment. The sequences were then merged into

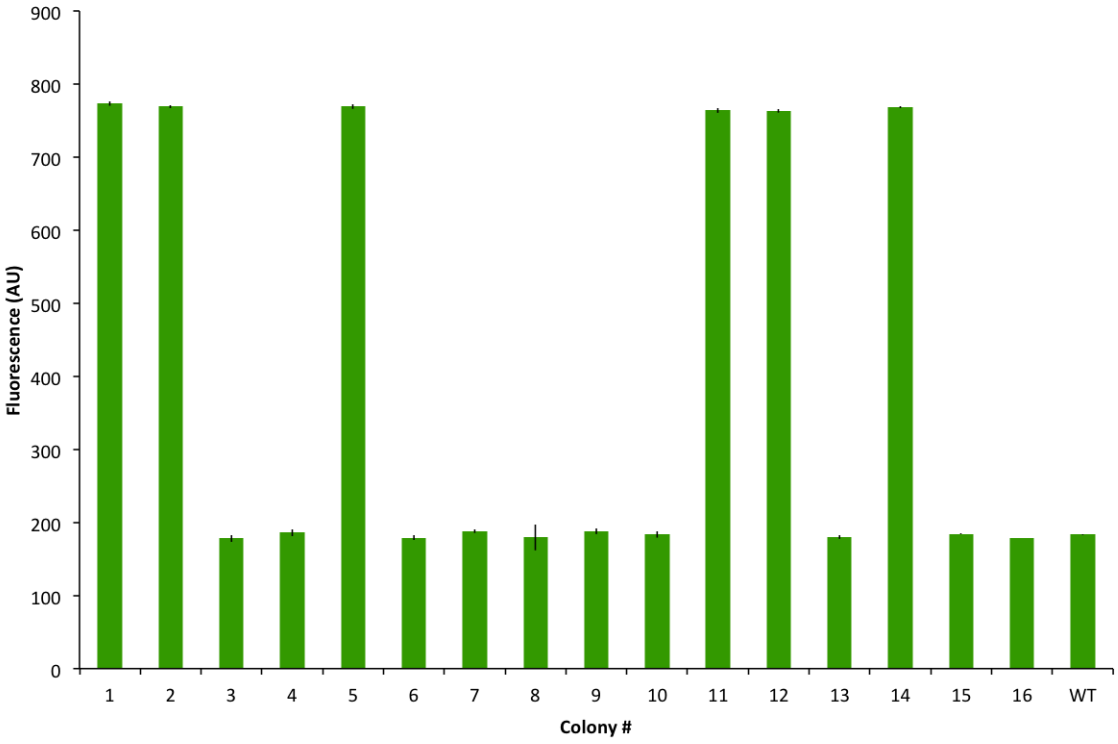

Figure 3.7 GFP fluorescence analyzed by flow cytometry for the 16 YBA3 colonies and wild type BY4742. Cells were streaked from glycerol stock onto YPD + G418 plates and grown for two days. Single colonies were innoculated into 2 mL of YPD + 2% glucose + 2% adenine and grown overnight. Overnight cultures were reinnoculated in 400 μL of yeast synthetic complete media + 2% glucose + 2% adenine to a cell density of 0.153×10^7 cells/mL and grown for 3 hours. Cultures were then analyzed on the flow cytometer. 3 technical replicates of each sample were measured and an autogate was used to keep 75 % of the collected data. Mean fluorescence for each colony is graphed and error bars show the standard deviation.

Table 3.2 The number, name, and binding position of primers used for sequencing the YBA3 constucts. Primer bidning sights are roughly spaced in 500 bp increments.

Number	Primer	Position
1	R32	14
2	R44	577
3	R45	926
4	R46	1332
5	R33	1816
6	R34	2406
7	R35	2951
8	R36	3218
9	R37	3765

a single sequence, in the case of overlapping reads, the nucleotide more similar to the reference sequence was chosen. A multiple alignment of the composite sequence to the reference sequence was performed for each colony. The sequencing reactions achieved approximately 60 % coverage across all YBA3 colonies. All mismatches were analyzed manually by looking at the chromatographs, and 7 definitive mutations were identified. This corresponds to a mutation rate of 0.000175 mutations per nucleotide synthesized. Of these mutations, 4 occurred at the junction of Ura3 and GFP.

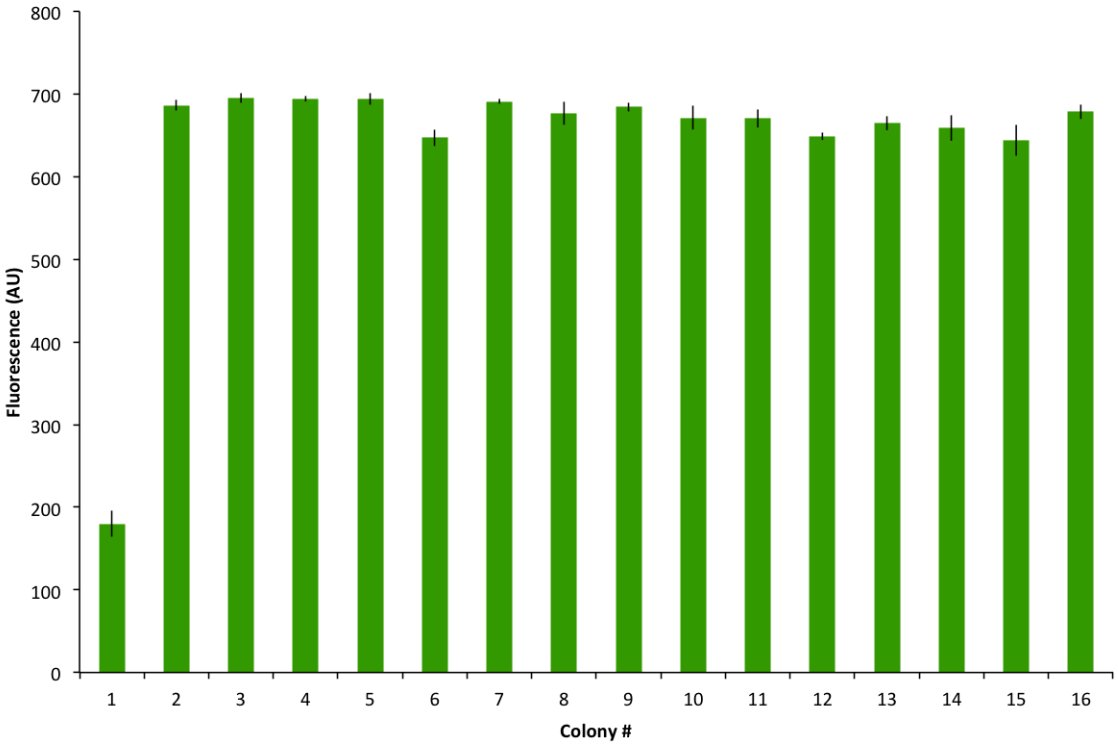

Figure 3.8 GFP fluorescence analyzed by flow cytometry for the 16 YBA3T colonies. Cells were streaked from glycerol stock onto YPD + G418 plates and grown for two days. Single colonies were innoculated into 2 mL of YPD + 2% glucose + 2% adenine and grown overnight. Overnight cultures were reinnoculated in 400 μL of yeast synthetic complete media + 2% glucose + 2% adenine to a cell density of 0.153×10^7 cells/mL and grown for 3 hours. Cultures were then analyzed on the flow cytometer. 3 technical replicates of each sample were measured and an autogate was used to keep 75 % of the collected data. Mean fluorescence for each colony is graphed and error bars show the standard deviation.

Table 3.3 The number, name, primers, and size of each part used in the YBA3T construction.

ID	Part	FP	RP	Size (bp)	Source
T	Trp1	T70	T71	674	pRS403
3T	TDH3-Trp1	M28	T71	1399	
T5	Trp1-GFP	T70	K60	1388	

3.2 BrickMason v2.0 protocol

3.2.1 YBA3T construction and screening

The majority of errors in the YBA3 assembly occurred at the junction between Ura3 and GFP, we decided to address the problem with the BrickMason v2.0 protocol. To demonstrate the advantages of this protocol, we reconstructed YBA3 with a Trp1-GFP fusion in place of the Ura3-GFP fusion, this construct was named YBA3T. The Trp1 gene was chosen for the assembly since it has an illegal XbaI site which would prevent it from being used in a standard BioBrick assembly. The assembly of the Trp1-GFP fusion is described in table 3.3, the rest of the dimers were taken from the original YBA3 assembly. A final BrickMason v2.0 reaction was performed with precycling, and the final construct was transformed into BY4742. 16 colonies were chosen for screening by flow cytometry. 15 out of 16 colonies expressed GFP as shown in figure 3.8, this resulted in a 94% success rate. The construction of YBA3T and its screening by flow cytometry was conducted by Alex Power, this data is included in this thesis with his permission.

3.2.2 Assembly of YBA39

The remaining constructs in this thesis were entirely constructed using the BrickMason v2.0 protocol. A detailed assembly of YBA39 is presented in order to exemplify a typical assembly, the remaining constructs will be presented briefly without the accompanying gel pictures.

The YBA39 construct contains a TetR-BFP-Cyc8 fusion driven by the TDH3-LO promoter. It has a NatMX selection marker (providing resistance to Nourseothricin (ClonNat)) and is flanked by Ade2 landing pads. Dimers were PCR amplified from already existing constructs in our in-house BioBrick library using the primers listed in table 3.4 and were run on a gel as show in figure 3.9. These dimers were column purified and pooled into a final PCR reaction. They were precycled for 10 cycles before adding primers N11 and L3 and cycling for an additional 25 cycles. The final YBA39 fragment was transformed into BY4742 yeast cells and plated on YPD + 100 μg/mL Nourseothricin (ClonNat). A genomic extraction was performed on a colony chosen from the transformation plate. The genomic DNA was PCR amplified with N11 and L3, and the resulting fragment is 6766 bp and can be seen on the gel shown in figure 3.10.

3.3 Construction of gene regulatory network for the measurement of gene regulatory functions

The BrickMason v2.0 cloning method was used to build the gene regulatory network shown in figure 3.11. The purpose of this network is to measure GRFs for the promoter that is driving GFP expression. The GRF can be measure by using IPTG to vary the levels of the BFP tagged TF and recording the effect on GFP.

Table 3.4 The number, name, primers, and size of each dimer used in the YBA39 construction.

Number	Part	FP	RP	Size (bp)
1	Ade2-Nat-TPGK1	N11	U12	1590
2	TPGK1-TDH3-LO	T21	U51	918
3	TDH3-LO-TetR	T59	U26	1352
4	TetR-BFP-Cyc8a	V16	V36	2035
5	Cyc8abc	T33	U27	2901
6	Cyc8c-Ade4	V37	L3	909

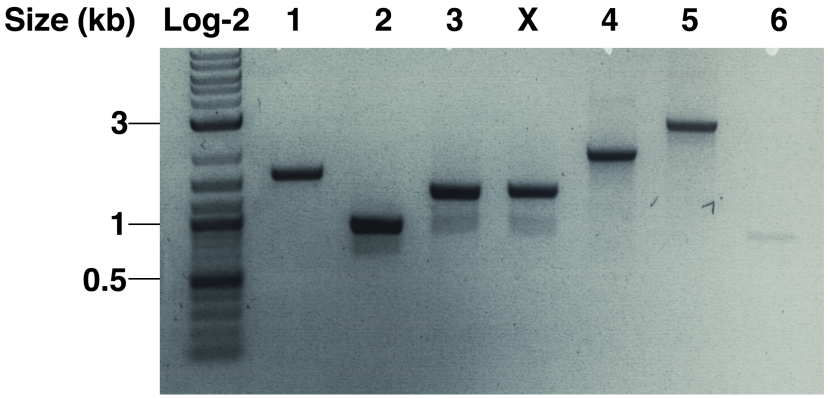

Figure 3.9 Dimers 1-6 used in the assembly of YBA39. The brightest band in each lane corresponds to the correct DNA fragment. These fragments were column purified and were used to assemble the final YBA39 construct using BrickMason v2.0.

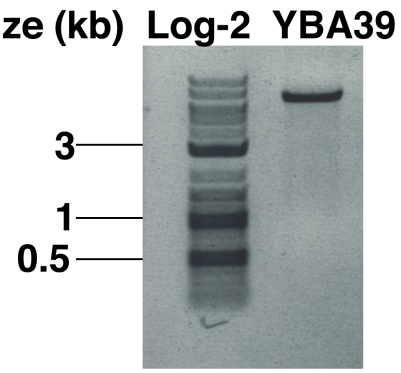

Figure 3.10 The final 6766 bp YBA39 construct was amplified from genomic DNA by PCR using primers N11 and L3

The network is composed of 3 constructs which are each integrated at a different locus. The *GAL4* locus contains the YBA28 construct which consists of constitutively expressed GEV and LacI proteins. The *ADE4* locus contains the YBA30 or 39 constructs which consist of the BFP tagged TF of interest whose expression is driven by a LacI repressed promoter. The *ADE2* locus contains the YBA27 or YBA35 construct which consists of the promoter of interest.

Details about the construction of YBA27-YBA39 can be found in tables 3.6-3.9 and table 3.4. An overview of these constructs is shown in table 3.5. The YBA27 and YBA35 constructs only differ in the promoter driving GFP expression. rMTGal1 contains TetR operator sites in the proximal region, and this represents a natural yeast repression mechanism. Gal1TX contains two TetR operator sites downstream from the TATA box, and this represents a steric hindrance mechanism of repression. Details about the construction of these synthetic promoters is included below. YBA30 and YBA39 only differ in the expressed repressor protein. YBA30 contains TetR-BFP-Cyc8 and YBA39 contains TetR-BFP, these proteins represent yeast natural and steric hindrance mechanisms of repression respectively.

Strains YBA56-YBA59 contain all the possible combinations of these promoters

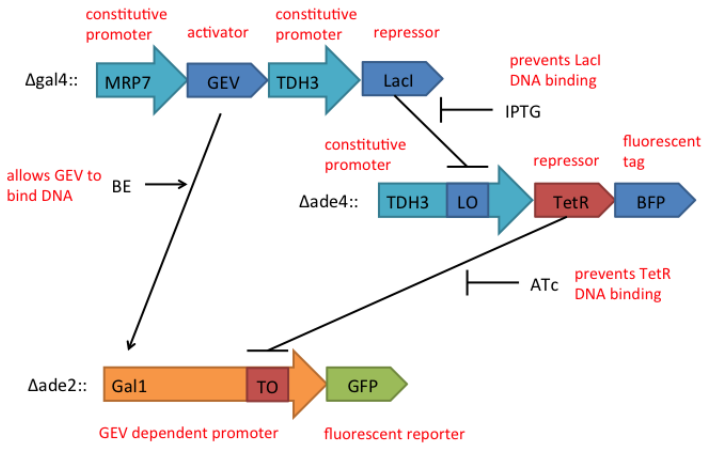

Figure 3.11 GEV is a β-estradiol (BE) dependent activator that can drive expression from Gal1 promoters. MRP7 and TDH3 are constitutive promoters. LacI can bind to the LacI operator sites in the TDH3-LO promoter. TetR can bind to the TetR operator sites in the Gal1 promoter. LacI and TetR binding can be inhibited by IPTG and ATc respecively. The network is divided into 3 constructs, each integrated into the same BY4742 strain at the indicated locus.

and repressors within the GRF network topology. An overview of the strains can be found in table 3.10. The strains were constructed by first integrating the construct at *ADE2*, followed by the construct at *GAL4*, and finally the construct at *ADE4*. *ADE2* was the first locus targeted for integration to enable easy colour screening. *GAL4* was the next locus used for integration since we could screen for successful transformants by measuring the GFP response to β-estradiol (BE). *ADE4* was the final construct targeted since we could now screen for white colonies.

Table 3.5 Strains constructed using the network design shown in figure 3.11. The corresponding repressor and promoter are listed.

Construct	Description	Locus
YBA27	Ade2 up-KanMX-rT_{ACT1}-$P_{rMTGal1}$-GFP-Ade2 down	*ADE2*
YBA35	Ade2 up-KanMX-rT_{ACT1}-P_{GalTX}-GFP-Ade2 down	*ADE2*
YBA28	His3-P_{MRP7}-GEV-T_{PGK1}-P_{TDH3}-LacI-T_{FBA1}	*GAL4*
YBA30	Ade4 up-NatMX-$P_{TDH3-LO}$-TetR-BFP-Cyc8-Ade4 down	*ADE4*
YBA39	Ade4 up-NatMX-$P_{TDH3-LO}$-TetR-BFP-Ade4 down	*ADE4*

Table 3.6 YBA27 construction details. Fragments 1 through 5 were amplified using the indicated primers, they were subsequently used to assemble the 12, 23, and 34 dimers. The final construct was created by combining 12-23-34-5 into a final PCR reaction.

Number	Description	FP	RP	Size (bp)
1	Ade2 up - KanMX	P34	K61	1664
2	rT_{ACT1}	T26	T25	293
3	$P_{rMTGal1}$	T27	H50	475
4	GFP	K59	K60	714
5	GFP-Ade2 down	K59	R57	999
12	Ade2 up-KanMX-rT_{ACT1}	P34	T25	1963
23	rT_{ACT1}-$P_{rMTGal1}$	T24	H50	774
34	$P_{rMTGal1}$-GFP	T27	K60	1195

Table 3.7 YBA35 construction details. Fragments 1,2, and 3 were amplified using the indicated primers, fragments 2 and 3 were assembled into a dimer. Fragment 1 and 23 share the rTACT1 homology and were assembled in a final PCR reaction.

Number	Description	FP	RP	Size (bp)
1	Ade2 up - KanMX-rT_{ACT1}	P34	U24	1963
2	P_{Gal1TX}	T26	U25	800
3	GFP-Ade2 down	V21	R57	999
23	P_{Gal1TX}-GFP-Ade2 down	T26	R57	1805

Table 3.8 YBA28 construction details. Fragments 1, 2, 3, and 4 were amplified using the indicated primers. They were used to create the 12, 23, and 24 dimers. These dimers were assembled in a final PCR reaction to create the final construct.

Number	Description	FP	RP	Size (bp)
1	His3-GEV-T_{PGK1}	T11	U12	3199
2	P_{TDH3}	T59	U51	725
3	LacI	T60	T62	1080
4	T_{FBA1}	T61	T13	
12	His3-GEV-T_{PGK1}-P_{TDH3}	T11	U51	3924
23	P_{TDH3}-LacI	T59	T62	1805
34	LacI-T_{FBA1}	T60	T13	1381

Table 3.9 YBA30 construction details. Fragments 1, 2, 3, 4, and 5 were amplified using the indicated primers. They were used to create the 12, 23, and 34 dimers. These dimers and fragment 5 were pooled into a final PCR reaction to create the final construct.

Number	Description	FP	RP	Size (bp)
1	Ade4 up-NatMX	N11	K61	1396
2	T_{PGK1}	T21	U12	193
3	$P_{TDH3-LO}$	T59	U51	725
4	TetR	V16	U26	621
5	TetR-BFP-Ade4 down	V16	L3	1544
12	Ade2-NatMX-T_{PGK1}	N11	U12	1590
23	T_{PGK1}-$P_{TDH3-LO}$	T21	U51	918
34	$P_{TDH3-LO}$-TetR	T59	U26	1352

Table 3.10 Strains constructed using the network design show in in figure 3.11. The corresponding repressor and promoter are listed

Strain	Repressor	Promoter
YBA56	TetR-BFP (YBA30)	rMTGal1 (YBA35)
YBA57	TetR-BFP (YBA30)	Gal1TX (YBA27)
YBA58	TetR-BFP-Cyc8 (YBA39)	rMTGal1 (YBA35)
YBA59	TetR-BFP-Cyc8 (YBA39)	Gal1TX (YBA27)

3.4 Construction of rMTGal1, Gal1TX, and TDH3LO promoters

rMTGal1, Gal1TX, and TDH3-LO are the 3 synthetic promoters used in this study. Both rMTGal1 and Gal1TX promoters are activated by the GEV in response to BE. The two Mig1 binding sites in the natural Gal1 promoter were replaced with TetR operator sites, this promoter was named rMTGal1. The Gal1TX promoter has the same Mig1 sites replaced with random sequences of the same length as the TetR operator site. It also has a TetR operator site inserted 15 bp downstream from the Gal1 TATA box. rMTGal1 represents natural mechanisms of yeast repression, and Gal1TX represents steric hindrance based repression. Gal1 and Gal10 are part of a naturally occurring divergent promoter and as a result they share the same UAS. To isolate the Gal1 promoter, our Gal1 promoters contain a reversed ACT1 terminator adjacent to the UAS. TDH3 promoter is a constitutive promoter, we inserted a LacI operator site 15 bp downstream from the TATA box and named this promoter TDH3-LO.

rMTGal1 was constructed by replacing the Mig1 sites in the wild type Gal1 promoter with TetR operator sites. The Gal1 promoter was split into 3 fragments, upstream of the first Mig1 site, between the Mig1 sites, and downstream of the second Mig1 site. The middle piece was ordered as a 64 bp oligo, a list of primers can be found in table 3.11. Each piece has a 20 bp overlap with its neighbours and was assembled using BrickMason v2.0. Gal1TX was constructed similarly, except the Mig1 sites were replaced by random sequences the same size as the TetR operator. The downstream fragment was PCR amplified from the already existing GalTX promoter from the pTPGI plasmid [11]. Details about the Gal1TX construction are shown in table 3.12.

Table 3.11 The number, name, primers, and size of each part used in the construction of the rMTGal1 promoter. Part 2 is a 64 bp oligo that shares 20 bp overlap with parts 1 and 3.

Number	**Part**	**FP**	**RP**	**Size (bp)**
1	rMTGal1 up	S24	T34	398
2	S34 (primer)			64
3	rMTGal1 down	T35	S25	188
123	$P_{rMTGal1}$	S24	S25	668

Table 3.12 The number, name, primers, and size of each part used in the construction of the Gal1TX promoter. Part 2 is a 64 bp oligo that shares 20 bp overlap with parts 1 and 3.

Number	**Part**	**FP**	**RP**	**Size (bp)**
1	rT_{ACT1}-Gal1TX up	T26	U62	514
2	S34 (primer)			64
3	Gal1TX down	U63	U25	184
123	rT_{ACT1}-P_{Gal1TX}	T26	U25	800

TDH3LO was created by inserting a LacI operator site 15 bp downstream from the TATA box. The TDH3 promoter was split into two fragments, downstream of the operator insertion and upstream of the operator insertion site. The LacI operator was introduced as a primer overhang on the reverse primer of the upstream fragment and the forward primer of the downstream fragment. The operator site served as the homology between the two fragments which were also assembled using BrickMason v2.0, details about primers and fragment sizes are shown in table 3.13.

Table 3.13 The number, name, primers, and size of each part used in the construction of the TDH3LO promoter.

Number	Part	FP	RP	Size (bp)	Source
1	TDH3LO up	T59	T57	642	BY4742
2	TDH3LO down			118	BY4742
12	TDH3LO	T59	U51	725	

3.5 Comparison of eukaryotic and prokaryotic mechanisms of repression

In order to generate GRFs for each strain, we performed a 2D ATc vs IPTG dose response curve. 8 concentrations of IPTG were used ranging from 0 mM to 10 mM, and 11 ATc concentrations were used ranging from 0 ng/mL to 150 ng/mL. 500 nM β-Estradiol was used as the inducing concentration for maximum activation of the Gal based promoter. Therefore 88 measurements were recorded for a single strain in a single dose response experiment. It was important to measure the GRN in the steady state. We adapted a previously described protocol [35] that allowed the cells to achieve a large number of cell divisions before measurement. This ensured that the measurements would be taken at steady state. Single colonies were inoculated into SC + 2% glucose overnight. The overnight cultures were re-diluted in SC + 2% glucose and grown for another 12 hours to each an OD_{600} of 0.2. The cells were then diluted 1/500 into the inducing media (SC + 2% glucose with the desired concentrations of IPTG, BE, and ATc). The cells were grown until they reached an OD_{600} of 0.6 (˜16-20 hours). They were subsequently diluted 1/2 in water before measurement by flow cytometry.

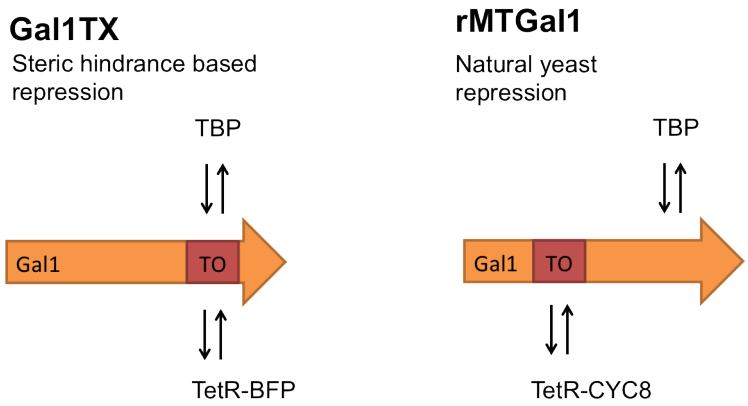

Figure 3.12 The Gal1TX promoter was obtained from a previous study [11], it contains two tandem TetR operator sites 11 bp after the TATA box. The rMTGal1 promoter was constructed in this study by replacing the two Mig1 operator sites in the wild type Gal1 promoter with TetR operator sites. Gal1TX represents a yeast steric hindrance repression mechanism and prevents the binding of TBP. rMTGal1 represents a natural yeast repression mechanism and does not prevent TBP from binding to the DNA.

The dose response curves were graphed and this data is shown in figures 3.14 - 3.17. The dose response experiment was repeated with different concentrations of BE for strain YBA58 as shown in figure 3.18.

3.6 BFP as a reporter

Figure 3.13 shows the 2D ATc vs IPTG dose response curve for strain YBA59 using GFP and BFP as reporters. IPTG concentrations are not shown on the graph, the repressor concentration is represented by BFP fluorescence. Data points are connected in order of increasing IPTG concentrations. We expect an increase in IPTG to result in an increase in BFP fluorescence, which should result in a decrease in GFP fluorescence. We can see that generally, an increase in BFP fluorescence results in a decrease in GFP fluorescence. However, an increase in IPTG concentration does not always result in an increase in BFP fluorescence as can be seen in the first two data

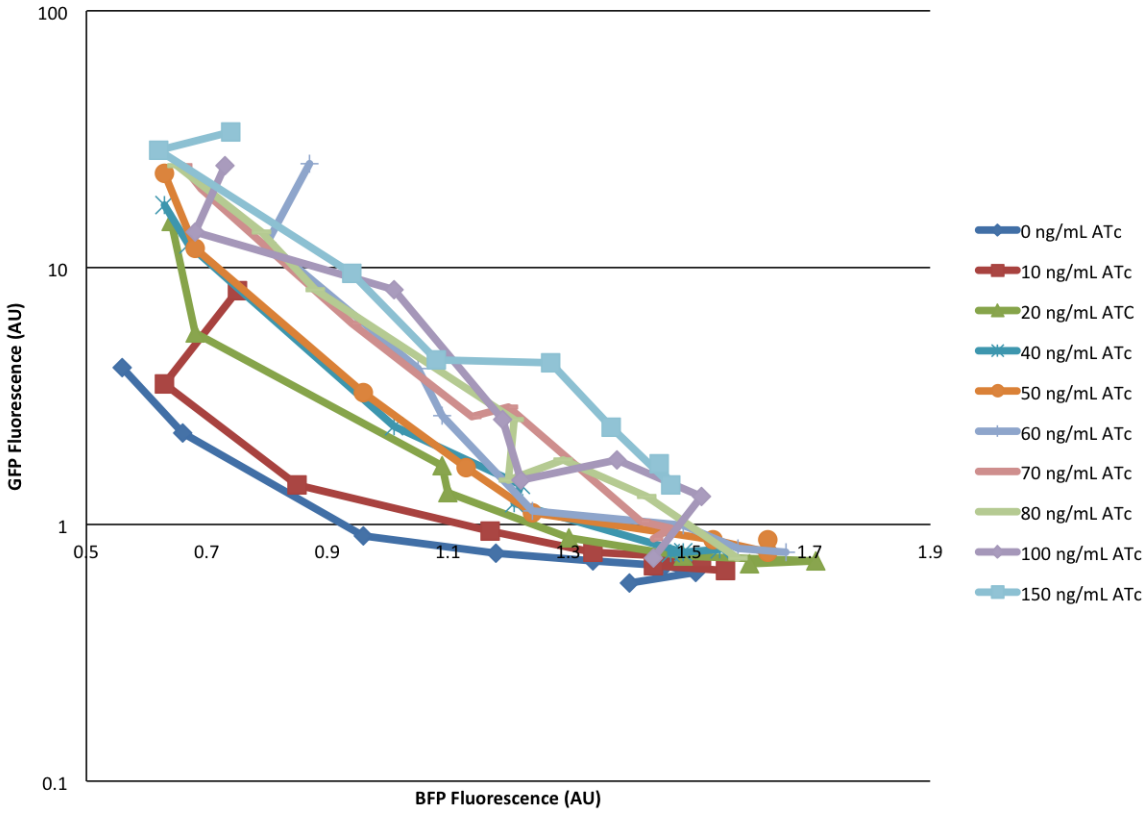

Figure 3.13 YBA59 2D ATc vs IPTG dose response experiment measured with 500 nM β-Estradiol. GFP fluorescence is plotted against IPTG concentration (0-10 mM) across various ATc concentrations (0-150 ng/mL).

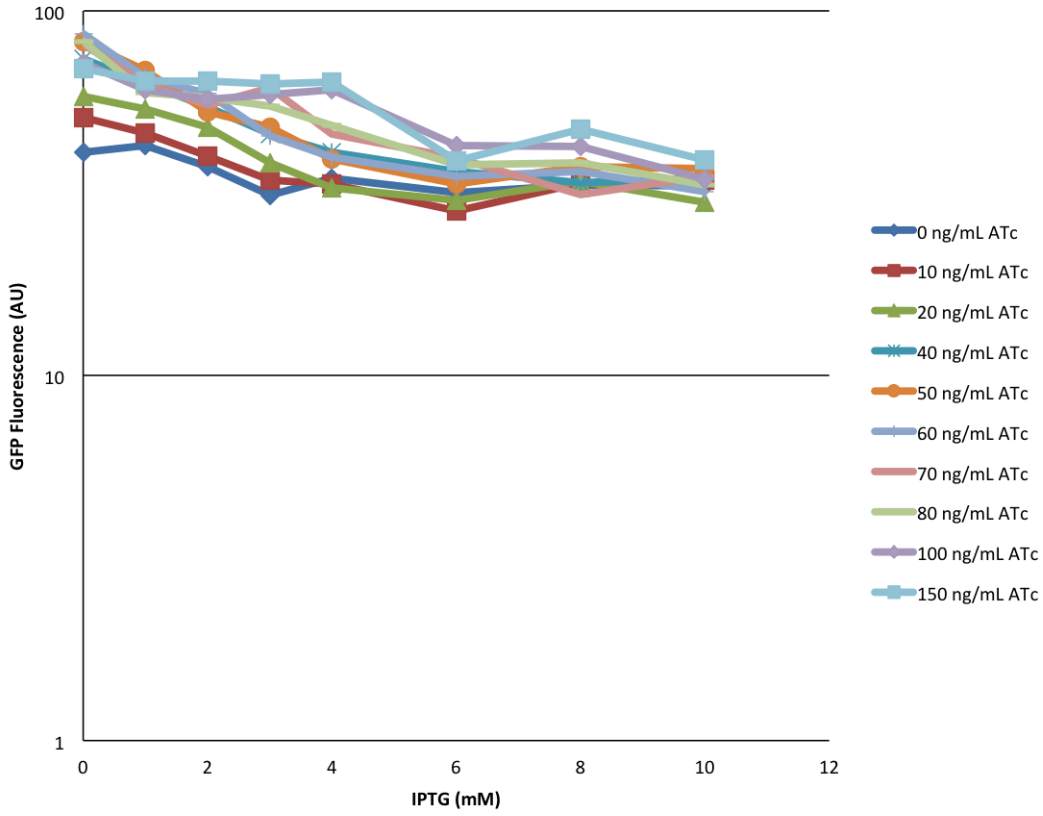

Figure 3.14 YBA56 2D ATc vs IPTG dose response experiment measured with 500 nM β-Estradiol. GFP fluorescence is plotted against IPTG concentration (0-10 mM) across various ATc concentrations (0-150 ng/mL).

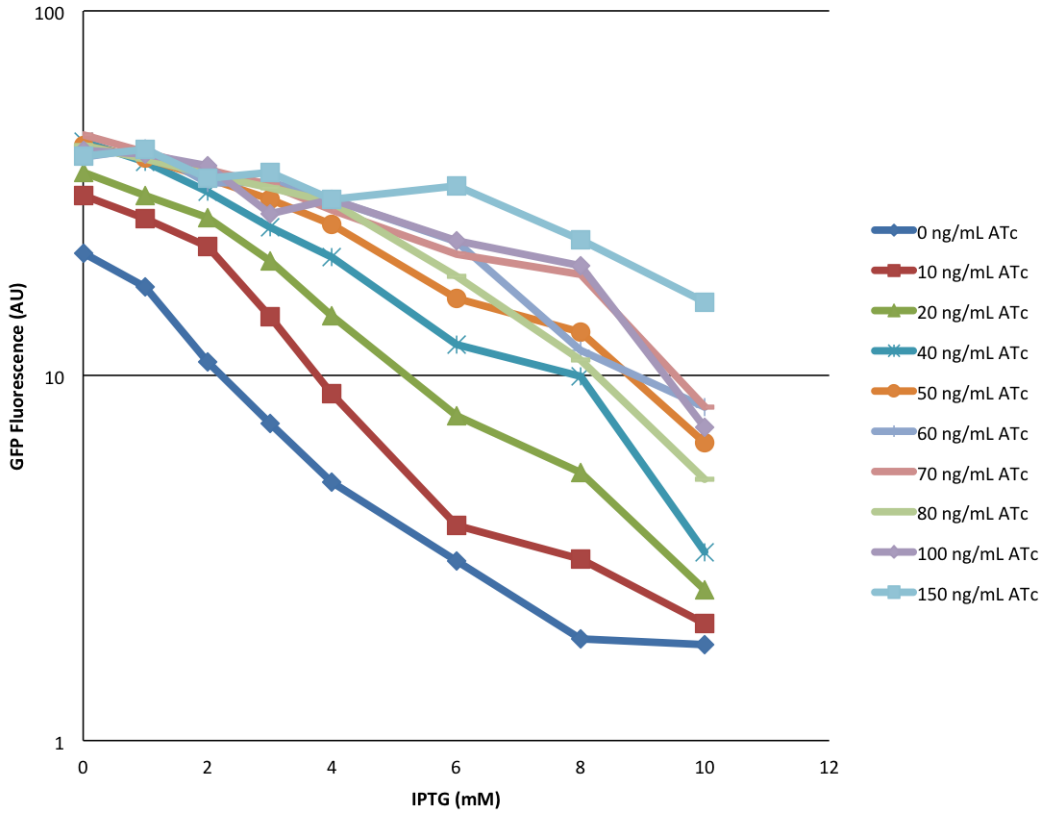

Figure 3.15 YBA57 2D ATc vs IPTG dose response experiment measured with 500 nM β-Estradiol. GFP fluorescence is plotted against IPTG concentration (0-10 mM) across various ATc concentrations(0-150 ng/mL).

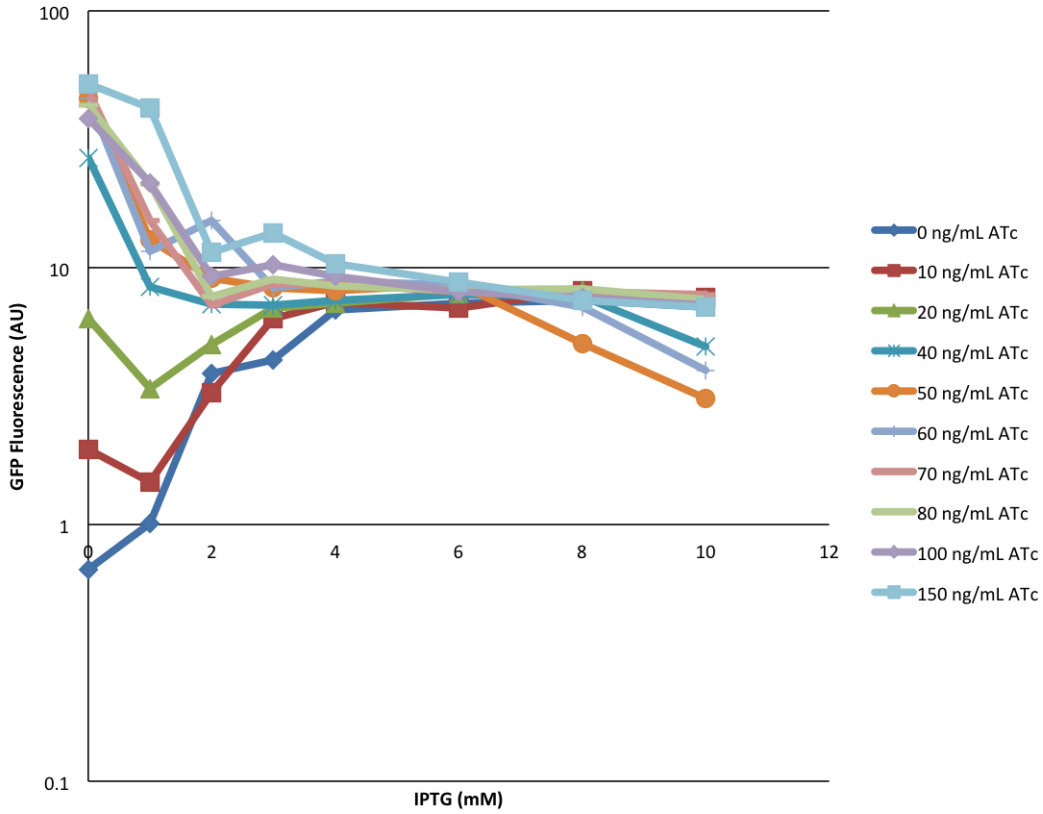

Figure 3.16 YBA58 2D ATc vs IPTG dose response experiment measured with 500 nM β-Estradiol. GFP fluorescence is plotted against IPTG concentration (0-10 mM) across various ATc concentrations (0-150 ng/mL).

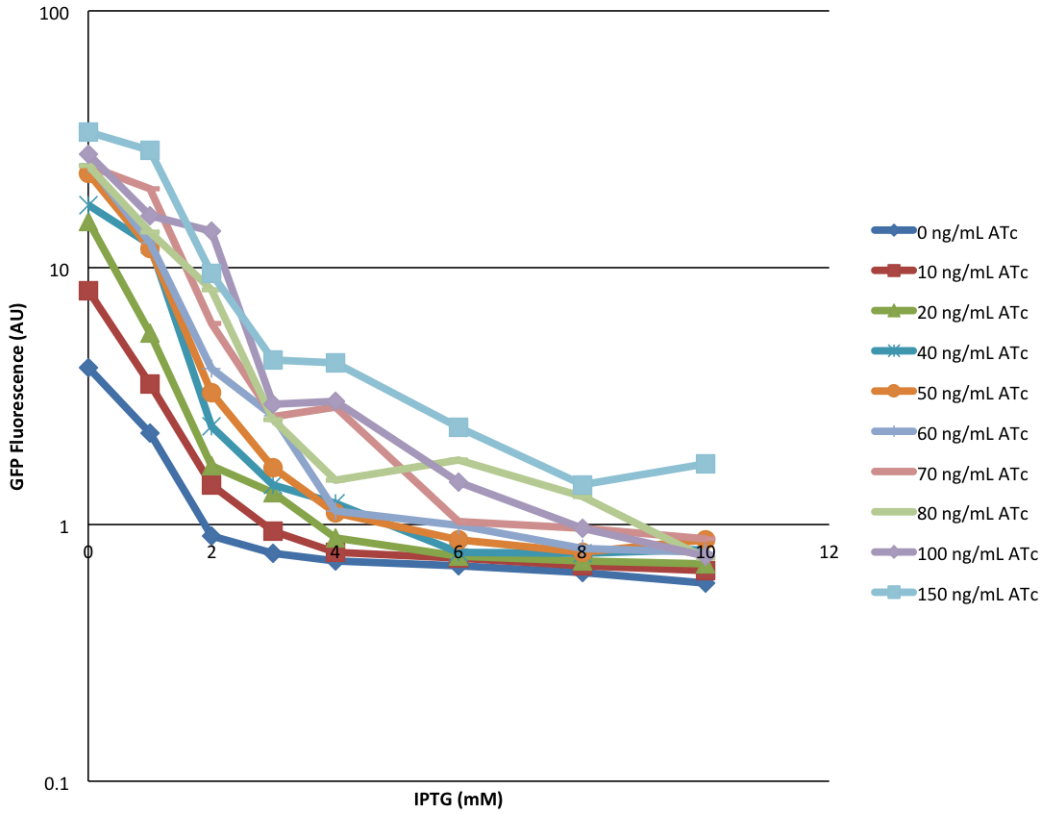

Figure 3.17 YBA59 2D ATc vs IPTG dose response experiment measured with 500 nM β-Estradiol. GFP fluorescence is plotted against IPTG concentration(0-10 mM) across various ATc concentrations (0-150 ng/mL).

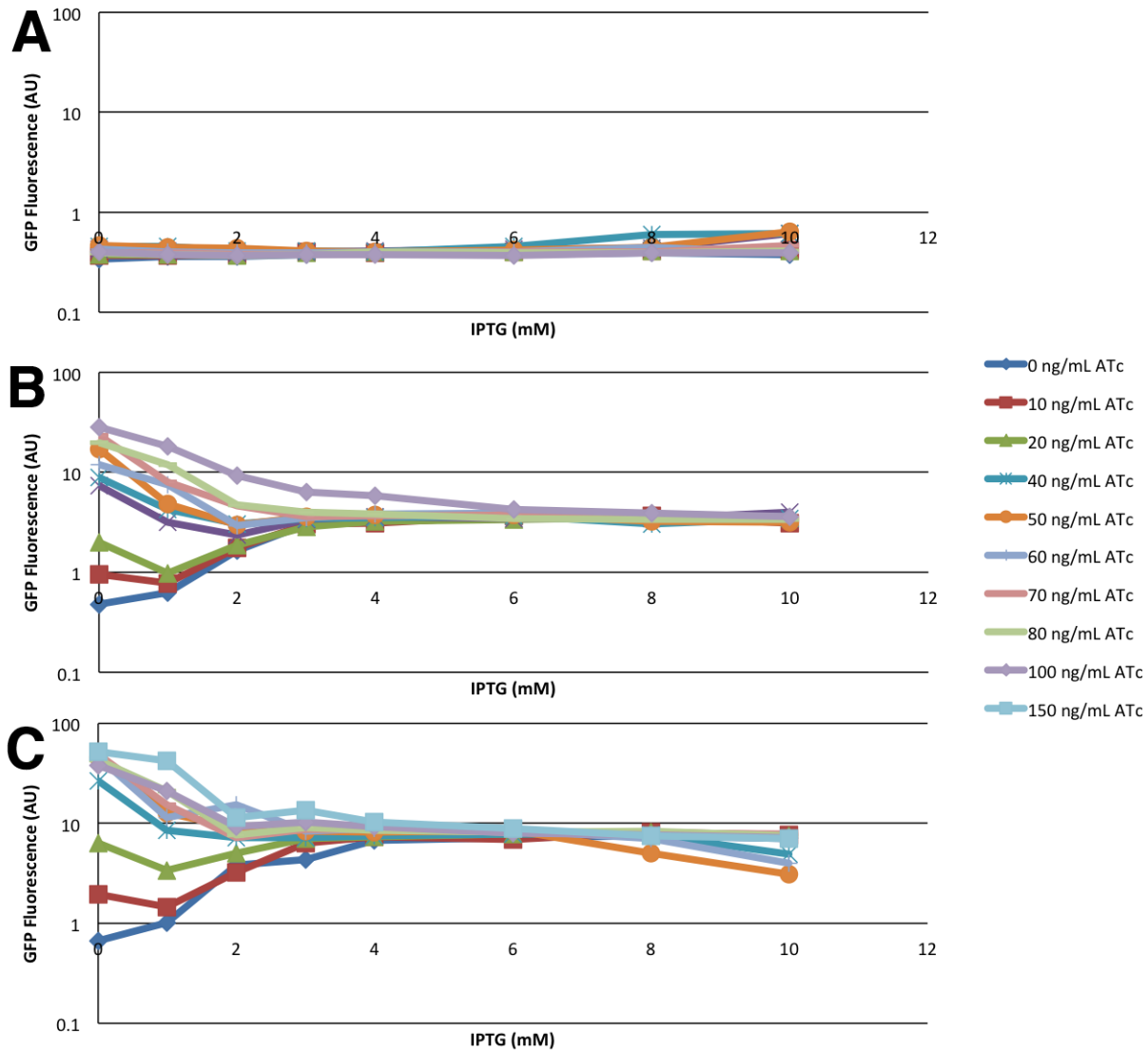

Figure 3.18 YBA58 2D ATc vs IPTG dose response experiment measured with (**A**) 0 nM, (**B**) 100 nM, and (**C**) 500 nM β-Estradiol. GFP fluorescence is plotted against IPTG concentration (0-10 mM) across various ATc concentrations (0-150 ng/mL).

points of the 150 ng/mL ATc curve. This is not a possible scenario in the context of the network architecture, as a result we believe that this effect is due to a noisy BFP signal. The same data is plotted using IPTG to represent the amount of repressor molecules present in the cell in figure 3.17. Here we can see the expected relationships, where an increase in IPTG results in a decrease in GFP expression.

3.7 YBA56 strain 2D ATc vs IPTG dose response experiment

The YBA56 strain contains the TetR-BFP repressor and the rMTGal1 promoter. The results of the 2D ATc vs IPTG dose response experiment are shown in figure 3.14. When the ATc concentration is held constant at 0 ng/mL, an increase in IPTG concentration results in only a small decrease in GFP expression. A similar result is observed across all measured ATc concentrations. This means that an increase in repressor molecule number has little effect on GFP expression. These results are expected since the TetR-BFP repressor is binding upstream of the TATA box and cannot significantly repress at this location through the steric hindrance mechanism.

3.8 YBA57 strain 2D ATc vs IPTG dose response experiment

The YBA57 strain contains the TetR-BFP repressor and the Gal1TX promoter. The results of the 2D ATc vs IPTG dose response experiment are shown in figure 3.15. When the ATc concentration is held constant at 0 ng/mL, an increase in IPTG concentration results in a sigmoidal decrease in GFP expression. As ATc concentration

is increased, and the percentage of repressor molecules able to bind DNA decreases, and an increase in GFP expression is observed. These results are expected, since the YBA57 strain contains the steric hindrance repression mechanism that has been extensively used in yeast synthetic networks.

3.9 YBA58 strain 2D ATc vs IPTG dose response experiment

The YBA58 strain contains the TetR-BFP-SSN6 repressor and the rMTGal1 promoter. The results of the 2D ATc vs IPTG dose response experiment are shown in figure 3.16. In the absence of ATc and IPTG, the GFP expression is fully repressed. When ATc concentration is held constant at 0 ng/mL ATc, an increase in IPTG results in an increase in GFP expression until a certain threshold of 10 AU GFP is reached. This means that an increase in the number of TetR-BFP-SSN6 repressor molecules unexpectedly results in decreased repression of GFP. When ATc concentration is 40 ng/mL and higher, GFP is minimally repressed at 40 ng/mL. An increase in IPTG concentration results in a decrease in GFP expression until the same threshold of 10 AU GFP is reached. This means that an increase in repressor molecules results in a decrease in GFP expression when the ATC concentration is greater than 40 ng/mL, and an increase in GFP expression when the ATc concentration is less than 40 ng/mL.

3.10 YBA59 strain 2D ATc vs IPTG dose response experiment

The YBA59 strain contains the TetR-BFP-SSN6 repressor and the Gal1Tx promoter. The results of the 2D ATc vs IPTG dose response experiment are shown in figure 3.17. When the ATc concentration is held constant at 0 ng/mL, an increase in IPTG concentration results in a sigmoidal decrease in GFP expression. As ATc concentration is increased, and the percentage of repressor molecules able to bind DNA decreases, and an increase in GFP expression is observed. Compared to TetR-BFP repressor in the YBA57 strain, the TetR-BFP-SSN6 repressor achieves a greater degree of repression.

3.11 TetR-BFP-Cyc8 as an activator

A 2D ATc vs IPTG dose response experiment for strain YBA58 was performed at 0nM, 100 nM, and 500 nM β-Estradiol (BE) concentrations. These results are shown in figure 3.18. We can see that in the absence of BE, there is no GFP expression. However, when BE is present, GFP fluorescence can be recorded, and the level of GFP expression is BE dependent.

Chapter 4

Discussion

4.1 BrickMason v1.0

The major motivations behind the development of the BrickMason v1.0 assembly protocol were to develop a method for the rapid assembly of gene regulatory networks and their genomic integration into yeast. We also wanted to minimize the number of primers that would need to be ordered for the assembly of a network. The protocol is based on the BioBrick Assembly standard and a mixture of PCR, digestion, and ligation are used to assemble fragments. The protocol has many advantages over the standard BioBrick Assembly protocol. It only requires the use of two restriction enzymes and it is backwards compatible with existing BioBrick parts. The speed of assembly is greatly increased, a 6 part construct can be assembled in a day. This would have previously taken 9 days using standard cloning protocols. Only one pair of standard BioBrick primers has to be ordered for each part. This single primer pair can be used to assemble that part in any context and in any order.

The BrickMason v1.0 protocol heavily relies on the use of restriction enzymes that leave palindromic overhangs. This is a limitation of the XbaI and SpeI restriction

enzymes chosen for use in the BioBrick assembly standard. DNA fragments that have palindromic overhangs are just as likely to self ligate as they are to ligate to the intended target resulting in a large number of side reactions. Other cloning methods have used non-palindromic overhangs [67], but this was not a possible option since we wanted to comply with existing BioBrick standards. Many steps in the BrickMason v1.0 protocol are dedicated to minimizing the number of self ligations, or formation of homodimers. The dephosphorylation of a linear fragment of DNA removes the 5' phosphate, which is necessary for the successful ligation of that fragment. The dephosphorylation of part B prevents the formation of a part B homodimer. Since part B fragments can no longer be consumed in the formation of homodimers, more fragments are available for binding with part A fragments. By extension, this also reduced the number of part A homodimers. Part A cannot also be dephosphorylated, because the phosphate is needed for a successful ligation with part B. When part A and part B are ligated, they create a mixed site at their junction which is undigestable by either XbaI or SpeI. After the ligation reaction is completed, it can be treated with XbaI and SpeI to digest away any A homodimers, or the small number of B homodimers that may have formed. This digestion step will release part A and part B monomers and these fragments can be incorporated into the subsequent PCR reaction of the AB dimer. The final gel extraction step ensures that the AB dimer is the only final product.

A major rate limiting step in standard cloning techniques is the transformation of intermediate DNA fragments into *E. coli*. This step alone takes 3 days to complete, 1 day to transform the construct, 1 day to grow the cells on a selection plate, and 1 day to grow the cells for DNA harvesting. The BrickMason v1.0 protocol avoids the transformation step by assembling parts in vitro using PCR and digestion/ligation, which takes several hours to complete. By creating overlapping dimers, consecutive

dimers have hundreds base pairs of homology with their neighbours. This greatly increases the chances that only the correct fragments will bind to each other, as a result a larger number of pieces can be assembled in a single PCR reaction. For the genomic integration of the construct, the BrickMason v1.0 protocol also saves time by allowing for the direct insertion of the construct into the genome, bypassing the need to first introduce the fragment into a plasmid.

Initially we had concerns over the possibility of introducing mutations into the construct from multiple rounds of PCR. The sequencing results demonstrated that the number of mutations related to PCR was very low. Instead, the highest rate of mutation was related to the digestion and ligation of parts, and most errors occurred at the junction of two parts, Ura3 and GFP as described in our results. Nonetheless the 38% success rate obtained using BrickMason v1.0 is a significant improvement over conventional BioBrick assembly.

The primary motivation for the use of digestion/ligation enzymes in the BrickMason v1.0 protocol was to save costs on primers. We envisioned that only one set of standard BioBrick primers would be ordered for each part and this primer pair would allow this part to be assembled in any context and in any order. However, the low efficiency, high error rate, and additional steps related to digestion/ligation mean that these reactions often have to be repeated. The upfront cost of using digestion/ligation to assemble fragments may be lower, but the enzymes consumed in these reactions are non recoverable. The costs of repeating failed reactions quickly add up to being more expensive than ordering part specific primers in the first place. We decided to improve the BrickMason v1.0 protocol by circumventing the digestion/ligation steps.

4.2 BrickMason v2.0

Although the BrickMason v1.0 method is already a great improvement over traditional cloning and standard BioBrick assembly protocols, improvements in the efficiency of the protocol are necessary to make it practical for daily use. Specifically we chose to focus on minimizing the number of steps performed, decreasing the construction time, and improving the efficiency of the final construction. This led to the BrickMason v2.0 protocol.

An overview of the BrickMason v2.0 protocol is shown in figure 2.3. We chose to replace the digestion/ligation steps with overlap extension PCR [28] for assembling dimers. This allowed us to eliminate many steps from the protocol. The time to assemble a construct was cut in half and may be comfortably completed by one person in a single day. This modification also eliminates the need for gel extractions when forming dimers, making the process easier to automate. There are also no longer any restrictions imposed on part sequences and parts can be assembled without the introduction of scars. Since there are fewer steps in this new protocol, and each step is more efficient, the chances that an assembly fails is much smaller. Typically, the minimal amount of a primer that can be ordered is 25 nM. Approximately 25 pM of a primer is required for a single PCR reaction, a single primer order provides enough reagent for 100 reactions. Therefore reactions that do fail can easily be repeated without driving up the costs of the assembly.

The cost of an assembly can be minimized by maximizing the reusability of ordered primers, therefore we decided to standardize the design of BrickMason v2.0 primers. The reverse primer for each part in the assembly is only 25 bp long and is homologous to the last 25 bp of that part. The forward primer for a part has a 25 bp overhang homologous to the previous part in the assembly, followed by a 25 bp homology for

that part, this primer is also known as a linker primer. The reverse primers only need to be ordered once and are context independent. The researcher needs to order linker primers specific to a particular assembly.

By using PCR to assemble monomers, the linker primers become responsible for determining the order of the assembly. This allows the researcher to assemble up to 5 parts at a time, multimers can be created rather than only dimers. A thermocycling program known as pre-cycling is used to greatly increase the efficiency of a multimer assembly, and is also useful for the assembly of the finalized construct form multimers or dimers. 10 rounds of PCR are performed with a standard PCR mix excluding primers. This allows the DNA fragments to stitch together, and by the time the 10 rounds are done, there are likely some fully assembled fragments in the solution. Primers are added and a standard PCR reaction is performed, the final fragment will be present in the reaction mix and is ready for amplification. Any partial assemblies that exist in the sample will be incorporated into this PCR reaction.

4.3 Comparison to other assembly methods

The BrickMason v1.0 assembly protocol is a novel approach for the assembly of BioBrick parts, however, the digestion/ligation steps are too unreliable for this technique to be used on a daily basis. The BrickMason v2.0 is much more robust and allows for a faster assembly time. BrickMason v2.0 is similar to other assembly protocols described in the literature such as Gibson assembly and the DNA assembler. However, the BrickMason v2.0 protocol does have several advantages over these other methods. Firstly, since fragments are run on a gel, BrickMason v2.0 allows the researcher to easily troubleshoot the assembly. If a DNA fragment is faulty, it is easy to determine which one it is. This would be very difficult to identify in a reaction in which all the

components are pooled. BrickMason v2.0 also allows the researcher to try various assembly strategies, for instance when assembling a 6 gene network, the researcher can try assembling 3 dimers, or 1 dimer and 1 4-part multimer. There are many reasons why one strategy may work better than another, such as secondary structure formation or the melting temperature associated with part homologies. The Gibson assembly method may also run into problems when assembling smaller fragments. For example, a 100 bp DNA fragment could be easily digested by the T5 exonuclease to completion, resulting in a very low efficiency assembly. Small fragments are however well tolerated by the BrickMason v2.0 protocol.

In the DNA assembler method, homologous DNA fragments are simultaneously transformed into a yeast cell. The cell uses its native recombination machinery to assemble the final construct. Yeast are known to incorporate linear double stranded DNA into the genome with high efficiency through homologous recombination [49]. The transformed DNA fragments can just as easily integrate into the genome non specifically. This is especially concerning if native yeast parts are used in the assembly that have large homologies to the yeast genome. BrickMason v2.0 avoids such a situation since all parts are assembled in vitro and the final construct is transformed as a single piece.

We envision that the BrickMason v2.0 would fill a new role in the gene assembly landscape rather than competing with existing technologies. With its ability to assemble smaller pieces robustly, BrickMason could be combined with homologous recombination approaches to build large constructs. Many yeast promoters are only several hundred base pairs long, and the manipulation of small DNA fragments is necessary for the construction of promoter variants and the insertion of operator sites. DNA fragments generated through gene synthesis are typically less then 1 kb, and the synthesis of larger fragments becomes much more expensive. BrickMason could

be used to assemble fragments up to 10 kb, approaching the limits of in vitro PCR. DNA assembler could then be used to assemble several 10 kb fragments into the final construct in vivo.

4.4 Measurement of gene regulatory functions

The gene regulatory function is the quantitative relationship between transcription factor concentrations and the rate of protein production [56]. The network described in figure 3.11 was designed to enable the characterization of steric hindrance and natural yeast mechanisms of repression and was constructed using the BrickMason v2.0 protocol. Since the repressor in this network is tagged with BFP and the output promoter is tagged with GFP, a GRF can be constructed by measuring GFP fluorescence across varying BFP fluorescence. GRFs comparing these repression mechanisms have not been previously measured in the literature, and can provide insights into the differences between them.

GRF's for activators have been previously measured in yeast by fluorescent microscopy, using exposure times as long as 5 minutes [37]. We were interested in measuring GRFs in yeast by flow cytometry since it would allow for the collection of high throughput data. Figure 3.13 shows the GFP vs BFP GRF that was measured for the YBA59 strain. Although the BFP signal is detectable, it is weak and unreliable. In other studies, transcription factors are approximately 10-100 times less abundant than the output fluorescent protein [36,37]. We observed similarly low BFP levels as shown in figure 3.13.

The major reason for the poor signal quality of the BFP signal has to do with the high autofluorescence emitted by yeast during measurement by flow cytometry. Since the autofluorescence is high and the BFP signal is low, variation in the autoflu-

orescence signal can mask significant changes in the BFP signal. This effect can be observed in figure 3.13 by looking at the first two points of the 10 ng/mL curve (red). The measurements were taken in the presence of 0 mM and 1 mM IPTG respectively. Since IPTG is increasing from the first point to the second, we would expect less repression by LacI. This would result in an increase in BFP fluorescence and a decrease in GFP fluorescence. A decrease in GFP expression is observed, but a decrease in BFP expression is also observed, which is not a possibility in the network.

The same data is presented in figure 3.17 except the GFP fluorescence is plotted against IPTG concentrations. The data is much easier to interpret this way and GFP expression decreases as IPTG is increased for the first two points of the 10 ng/mL curve, as we would expect. IPTG concentrations are not a direct measure of the abundance of the repressor in the network. However, due to the high autofluorescence and the low signal intensity obtained from BFP fluorescence, IPTG is a better measurement. A problem associated with using IPTG concentrations to infer repressor abundance is that the relationship between IPTG concentration and BFP abundance is not necessarily linear. This can result from many factors such as variations in drug transport across the membrane [48]. Since the BFP signal is so unreliable, IPTG concentration is the best parameter to use for estimating repressor concentration. The same strains could be analyzed by fluorescent microscopy to get a better measurement of the BFP signal, however this would not allow for the collection of high throughput data. BFP and GFP were the only fluorescent markers that were compatible with our flow cytometer. BFP and GFP have a similar level of brightness, the weak BFP signal has to with the low expression levels of the tagged repressor protein. Even if it would be possible to use a different fluorescent marker with our system, it is unlikely to produce a signal significantly stronger than BFP.

4.5 Dynamic range

The Gal1TX and the rMTGal1 promoters only differ in the position of the TetR repressor binding site. It has been well documented in the past that promoter modifications near the proximal promoters of native yeast genes can lead to a reduction in expression from that promoter [11]. Our results suggest that changes to the promoter in the distal region appear to have less of an effect on expression. Strains YBA56 and YBA58 contain the TetR operator in the distal region and have higher maximum expression than strains YBA57 and YBA59. This result fits well with the model that yeast genes have a nucleosome free region in the distal promoter that is responsible for determining the state of the proximal promoter [41]. When activators bind in the nucelosome free region, the proximal promoter is cleared of any repressive chromatin structures. The primary role of the proximal promoter is to initiate transcription by precisely assembling the transcriptional machinery [61]. Therefore changes at the nucleosome free region are well tolerated but changes at the proximal promoter can interfere with the precise positioning of core transcription factors. From a synthetic biology design perspective, regulation at the distal promoter allows for a much larger dynamic range of expression since it does not reduce the maximum output of a promoter. This allows for the creation of synthetic networks with larger ranges of input and output.

4.6 Strength of repression

The binding of TetR to the operator sites in Gal1TX is thought to achieve repression by inhibiting the binding of TBP through steric hindrance. A comparison of figures 3.15 and 3.17 shows that when the TetR-BFP repressor is tagged with Cyc8, it becomes a much stronger repressor. The greater degree of repression could be a

result of many factors such as the localization of the repressor protein, the increased size of the repressor contributing to steric hindrance, or the potential for activating mechanisms of repression beyond steric hindrance. Of all these factors, we believe that the increased repression associated with TetR-BFP-Cyc8 at the Gal1TX promoter is predominantly a result of the nuclear localization of this protein. Although its nuclear localization has not been demonstrated experimentally, we believe it is highly likely since Cyc8-GFP localizes to the nucleus [31]. The yeast nucleus is estimated to occupy approximately 7% of the yeast cell [32]. A nuclear localization signal will compress the entire repressor content into the nucleus, increasing the effective repressor concentration by a factor of 14. Although the nuclear localization of TetR-BFP-Cyc8 needs to be proven experimentally, we hypothesize that it is the major factor responsible for the increased repression observed over TetR-BFP in the Gal1TX promoter. This hypothesis could be tested by tagging TetR-BFP with an NLS and comparing the repression to the TetR-BFP-Cyc8 repressor.

4.7 Evidence for different mechanisms of repression

It is unclear whether or not steric based repression mechanisms are equivalent to natural yeast mechanisms of repression. The construction and characterization of the YBA56-59 strains allowed us to perform a side by side comparison of both repression mechanisms. In strain YBA56, the rMTGal1 promoter is repressed by a TetR-BFP fusion protein. GFP expression decreases minimally with increasing IPTG concentrations. The relatively small degree of repression that is observed could be related to the decreased growth rate of yeast in the presence of IPTG. Alternatively, the TetR-BFP repressor may be able to prevent the binding of activating transcription

factors at the distal promoter. However if this were the case, we would expect a much higher degree of repression. The YBA58 strain only differs from YBA56 in that the repressor is tagged with Cyc8. Under the same conditions, YBA58 is able to achieve a much higher degree of GFP repression as seen in figure 3.16, even though both repressors bind to the same operator. We hypothesize that the increased repression observed is mainly due to the ability of Cyc8 to recruit Tup1, leading to the initiation of native yeast repression mechanisms. As observed in strain YBA57, TetR-BFP is able to achieve a significant amount of repression when acting on the Gal1TX promoter, and by tagging it with Cyc8, a greater degree of repression can be achieved. As previously discussed, we hypothesize that the NLS embedded in Cyc8 is largely responsible for the increased repression. We discard the possibility that natural yeast repression mechanisms play a significant role in repressing this promoter. Whatever effects the native yeast repression mechanisms may have at this location would be masked by the steric hindrance effects of the repressor since TBP recruitment is further up the chain of events leading to transcription. If each of these strains exhibited the same steric hindrance based mechanism of repression, then we would expect that introducing Cyc8 into YBA56 would have the same relative effect as its introduction into YBA57. This, however, is not the case; the introduction of Cyc8 into YBA56 causes the most weakly repressed network to become the most strongly repressed while completely changing the shape of the GRF. When it is introduced to YBA57, the shape of the GRF remains the same and strength of repression seems to increase by a consistent factor. At the Gal1TX promoter both TetR-BFP and TetR-BFP-Cyc8 achieve repression, presumably through steric hindrance. At the rMTGal1 promoter, repression cannot be achieved through steric hindrance alone. Cyc8 is required to achieve repression, this provides evidence that Cyc8 has a function beyond the steric hindrance of the promoter. Taken together this data provides evidence that steric

hindrance and natural yeast mechanisms of repression are not equivalent.

4.8 Derepression

The most surprising finding in this study has been the derepression of GFP expression observed in figure 3.16 by the YBA58 strain. The repression of rMTGal1 by TetR-BFP-Cyc8 is stronger than any other repressor/promoter combination analyzed in this study, and also has the highest dynamic range. At 0 mM IPTG, full repression of the rMTGal1 promoter is achieved. However, an increase in IPTG concentration, which is equivalent to an increase in the molecule number of the repressor, leads to derepression of the rMTGal1 promoter. In the presence of ATc concentrations $\geq$40 ng/mL an increase in IPTG concentrations by the same amount leads to greater repression of the rMTGal1 promoter. In both cases, the level of repression approaches a similar level of GFP expression with increasing IPTG concentrations, we will refer to this level as the baseline level. In the case of figure 3.16 this level is approximately 10 AU.

The Cyc8/Tup1 complex has been previously shown to be involved in the activation of core promoters [65]. To ensure that the observed derepression effect was a result of derepression rather than activation, the dose response experiment was repeated with various concentrations of β-Estradiol as shown in figure 3.18. If the effect was a result of activation by Cyc8, then we would expect to observe an increase in GFP expression at 0 nM β-Estradiol. At 0 nM β-Estradiol, GEV is not able to activate the promoter, and any observed activation would have to be attributed to the Cyc8/Tup1 complex. As shown in figure 3.18 A, no activation is observed in the absence of β-Estradiol and we can confirm that the effect is in fact derepression. We also found that the baseline level of expression is related to the concentration of

β-Estradiol, as is the maximum expression that can be achieved from the promoter across ATc concentrations.

Others have shown that Cyc8 can only achieve 4 fold repression in Tup1 deletion strains. The baseline level of repression is approximately 4 fold repression over the maximum expression from the promoter. We hypothesize that the derepression is a result of free floating repressor quenching the available Tup1 repressor. At 0 mM IPTG an optimal number of TetR-BFP-Cyc8 repressor molecules are present in the nucleus. Each repressor molecule is in a complex with 4 Tup1 molecules. As we increase the repressor molecule number, each repressor molecule is no longer bound to 4 Tup1 molecules. After a certain point, only a fraction of repressor molecules will be bound to Tup1 at all. Therefore as we increase the number of repressor molecules, the repression strength approaches that of a Tup1 deletion strain. At high ATc concentrations, none of the repressor is allowed to bind. Increasing the molecule number allows the protein to overcome the ATc concentration, but it can only reach the baseline, because there is also no Tup1 available for binding to the repressor molecules.

An alternate explanation for the derepression effect is the possible involvement of Cyc8 in prion formation, which has been well documented [52]. We believe that it is an unlikely explanation since prion formation was only induced when a glutamine-rich region of Cyc8 was overexpressed on a high copy plasmid. This differs from the current study, where the full version of Cyc8 was expressed, and was present at significantly lower levels due to genomic integration. The derepression effect is not observed in strain YBA59 which expressed the same repressor protein at similar levels. Therefore it is unlikely that the derepression effect has to do with the impaired binding of the repressor protein to DNA.

4.9 Different mechanisms of repression

Both TetR-BFP and TetR-BFP-Cyc8 can repress in the proximal region of a promoter, and produce a similarly shaped GRF. In the distal region, TetR-BFP is unable to achieve significant repression. When this same repressor is tagged with Cyc8, it can achieve very strong repression, and exhibits a unique gene regulatory function. We hypothesize that at the proximal region, both proteins repress through steric hindrance. At the distal region, steric hindrance no longer has a significant effect and repression can only be achieved through natural Cyc8 mediated yeast mechanisms. This evidence in this study demonstrates that repression through steric hindrance and natural mechanisms are not equivalent. We have yet to demonstrate that the TetR-BFP-Cyc8 acts just as a natural yeast repressor, however it is closer than steric hindrance repressors, which are rarely found in yeast. From a synthetic biology perspective, the Cyc8 based repression is stronger and can also achieve a higher dynamic range. It may also have some interesting applications in genetic circuit design. One example is as a noise filter, if ATc is a noisy input signal, IPTG can be used to regulate the noise of the output gene expression.

This study opens many avenues for exploration with this repression mechanism. It would be particularly interesting to examine the effects of Cyc8 based repression on noise and epigenetic memory. Many previous studies have used steric hindrance as opposed to natural yeast mechanisms of repression to study gene expression in eukaryotes. As a result, the conclusions from this work may have far reaching implications.

Bibliography

[1] G Bellí, E Gari, L Piedrafita, M Aldea, and E Herrero. An activator/repressor dual system allows tight tetracycline-regulated gene expression in budding yeast. *Nucleic Acids Research*, 26(4):942–947, February 1998.

[2] William J Blake, Gabor Balazsi, Michael A Kohanski, Farren J Isaacs, Kevin F Murphy, Yina Kuang, Charles R Cantor, David R Walt, and James J Collins. Phenotypic Consequences of Promoter-Mediated Transcriptional Noise. *Molecular Cell*, 24(6):853–865, December 2006.

[3] William J Blake, Mads KAErn, Charles R Cantor, and J J Collins. Noise in eukaryotic gene expression. *Nature*, 422(6932):633–637, April 2003.

[4] Dmitri Bratsun, Dmitri Volfson, Lev S Tsimring, and Jeff Hasty. Delay-induced stochastic oscillations in gene regulation. *Proceedings of the National Academy of Sciences of the United States of America*, 102(41):14593–14598, October 2005.

[5] R. Brent and M Ptashne. A bacterial repressor protein or a yeast transcriptional terminator can block upstream activation of a yeast gene. *Nature*, 312(5995):612–615, 1984.

[6] R. Brent and M Ptashne. A eukaryotic transcriptional activator bearing the DNA specificity of a prokaryotic repressor. *Cell*, 43(3 Pt 2):729–736, December 1985.

[7] D R Burrill and P A Silver. Synthetic circuit identifies subpopulations with sustained memory of DNA damage. *Genes and Development*, 25(5):434–439, March 2011.

[8] L. Campos. That was the synthetic biology that was. *Synthetic Biology*, pages 5–21, 2010.

[9] Barry Canton, Anna Labno, and Drew Endy. Refinement and standardization of synthetic biological parts and devices. *Nature Biotechnology*, 26(7):787–793, January 2008.

[10] Tom Ellis, Tom Adie, and Geoff S Baldwin. DNA assembly for synthetic biology: from parts to pathways and beyond. *Integrative Biology*, 3(2):109, 2011.

[11] Tom Ellis, Xiao Wang, and James J Collins. Diversity-based, model-guided construction of synthetic gene networks with predicted functions. *Nature Biotechnology*, 27(5):465–471, May 2009.

[12] M B Elowitz and S Leibler. A synthetic oscillatory network of transcriptional regulators. *Nature*, 403(6767):335–338, January 2000.

[13] Drew Endy. Foundations for engineering biology. *Nature*, 438(7067):449–453, November 2005.

[14] R H Fogh, G Ottleben, H Rüterjans, M Schnarr, R Boelens, and R Kaptein. Solution structure of the LexA repressor DNA binding domain determined by 1H NMR spectroscopy. *EMBO Journal*, 13(17):3936–3944, September 1994.

[15] Ari E Friedland, Timothy K Lu, Xiao Wang, David Shi, George Church, and James J Collins. Synthetic Gene Networks That Count. *Science (New York, NY)*, 324(5931):1199–1202, January 2009.

[16] T S Gardner, C R Cantor, and J J Collins. Construction of a genetic toggle switch in Escherichia coli. *Nature*, 403(6767):339–342, January 2000.

[17] K Gaston and P S Jayaraman. Transcriptional repression in eukaryotes: repressors and repression mechanisms. *Cellular and Molecular Life Sciences*, 60(4):721–741, 2003.

[18] D Gibson. Synthesis of DNA fragments in yeast by one-step assembly of overlapping oligonucleotides. *Nucleic Acids Research*, September 2009.

[19] Daniel G Gibson, Gwynedd A Benders, Cynthia Andrews-Pfannkoch, Evgeniya A Denisova, Holly Baden-Tillson, Jayshree Zaveri, Timothy B Stockwell, Anushka Brownley, David W Thomas, Mikkel A Algire, Chuck Merryman, Lei Young, Vladimir N Noskov, John I Glass, J Craig Venter, Clyde A Hutchison, and Hamilton O Smith. Complete chemical synthesis, assembly, and cloning of a Mycoplasma genitalium genome. *Science (New York, NY)*, 319(5867):1215–1220, February 2008.

[20] Daniel G Gibson, Lei Young, Ray-Yuan Chuang, J Craig Venter, Clyde A Hutchison, and Hamilton O Smith. Enzymatic assembly of DNA molecules up to several hundred kilobases. *Nature Methods*, 6(5):343–345, May 2009.

[21] B N G Giepmans, S R Adams, M H Ellisman, and R Y Tsien. The fluorescent toolbox for assessing protein location and function. *Science's STKE*, 312(5771):217, 2006.

[22] R D Gietz and R H Schiestl. High-efficiency yeast transformation using the LiAc/SS carrier DNA/PEG method. *Nature Protocols*, 2(1):31–34, 2007.

[23] M Gossen and H Bujard. Tight control of gene expression in mammalian cells by tetracycline-responsive promoters. *Proceedings of the National Academy of Sciences of the United States of America*, 89(12):5547, 1992.

[24] M Gossen, S. Freundlieb, G. Bender, G. Muller, W. Hillen, and H Bujard. Transcriptional activation by tetracyclines in mammalian cells. *Science (New York, NY)*, 268(5218):1766–1769, June 1995.

[25] M Gray and SM Honigberg. Effect of chromosomal locus, GC content and length of homology on PCR-mediated targeted gene replacement in Saccharomyces. *Nucleic Acids Research*, 29(24):5156–5162, January 2001.

[26] Kuk-Ki Hong, Wanwipa Vongsangnak, Goutham N Vemuri, and Jens Nielsen. Unravelling evolutionary strategies of yeast for improving galactose utilization through integrated systems level analysis. *Proceedings of the National Academy of Sciences of the United States of America*, 108(29):12179–12184, July 2011.

[27] Manqing Hong, Mary X Fitzgerald, Sandy Harper, Cheng Luo, David W Speicher, and Ronen Marmorstein. Structural basis for dimerization in DNA recognition by Gal4. *Structure (London, England : 1993)*, 16(7):1019–1026, July 2008.

[28] R M Horton, H D Hunt, S N Ho, J K Pullen, and L R Pease. Engineering hybrid genes without the use of restriction enzymes: gene splicing by overlap extension. *Gene*, 77(1):61–68, April 1989.

[29] Chieh Hsu, Simone Scherrer, Antoine Buetti-Dinh, Prasuna Ratna, Julia Pizzolato, Vincent Jaquet, and Attila Becskei. Stochastic signalling rewires the

interaction map of a multiple feedback network during yeast evolution. *Nature communications*, 3:682, 2012.

[30] MC Hu and N. Davidson. The inducible lac operator-repressor system is functional in mammalian cells. *Cell*, 48(4):555, 1987.

[31] W-K Huh, JV Falvo, LC Gerke, AS Carroll, RW Howson, JS Weissman, and EK O'Shea. Global analysis of protein localization in budding yeast. *Nature*, 425(6959):686–691, January 2003.

[32] Paul Jorgensen, Nicholas P Edgington, Brandt L Schneider, Ivan Rupes, Mike Tyers, and Bruce Futcher. The size of the nucleus increases as yeast cells grow. *Molecular biology of the cell*, 18(9):3523–3532, September 2007.

[33] C A Keleher, M J Redd, J Schultz, M Carlson, and A D Johnson. Ssn6-Tup1 is a general repressor of transcription in yeast. *Cell*, 68(4):709–719, February 1992.

[34] Jason R Kelly, Adam J Rubin, Joseph H Davis, Caroline M Ajo-Franklin, John Cumbers, Michael J Czar, Kim de Mora, Aaron L Glieberman, Dileep D Monie, and Drew Endy. Measuring the activity of BioBrick promoters using an in vivo reference standard. *Journal of biological engineering*, 3:4, January 2009.

[35] Harold D Kim and Erin K O'Shea. A quantitative model of transcription factor-activated gene expression. *Nature Structural and Molecular Biology*, 15(11):1192–1198, November 2008.

[36] Harold D Kim, Tal Shay, Erin K O'Shea, and Aviv Regev. Transcriptional regulatory circuits: predicting numbers from alphabets. *Science (New York, NY)*, 325(5939):429–432, July 2009.

[37] HD Kim and EK O'Shea. A quantitative model of transcription factor-activated gene expression. *Nature Structural and Molecular Biology*, 15(11):1192–1198, January 2008.

[38] Tom Knight. Idempotent Vector Design for Standard Assembly of Biobricks. *MIT Artificial Intelligence Laboratory; MIT Synthetic Biology Working Group*, pages 1–11, August 2003.

[39] Natalay Kouprina and Vladimir Larionov. Selective isolation of genomic loci from complex genomes by transformation-associated recombination cloning in the yeast Saccharomyces cerevisiae. *Nature Protocols*, 3(3):371–377, January 2008.

[40] MA Labow, SB Baim, T. Shenk, and AJ Levine. Conversion of the lac repressor into an allosterically regulated transcriptional activator for mammalian cells. *Molecular And Cellular Biology*, 10(7):3343–3356, 1990.

[41] Bing Li, Michael Carey, and Jerry L Workman. The Role of Chromatin during Transcription. *Cell*, 128(4):707–719, February 2007.

[42] Mamie Z Li and Stephen J Elledge. Harnessing homologous recombination in vitro to generate recombinant DNA via SLIC. *Nature Methods*, 4(3):251–256, March 2007.

[43] J F Louvion, B Havaux-Copf, and D Picard. Fusion of GAL4-VP16 to a steroid-binding domain provides a tool for gratuitous induction of galactose-responsive genes in yeast. *Gene*, 131(1):129–134, September 1993.

[44] Timothy K Lu, Ahmad S Khalil, and James J Collins. Next-generation synthetic gene networks. *Nature Biotechnology*, 27(12):1139–1150, December 2009.

[45] C Mateus and SV Avery. Destabilized green fluorescent protein for monitoring dynamic changes in yeast gene expression with flow cytometry. *Yeast*, 16(14):1313–1323, January 2000.

[46] D Mumberg, R Müller, and M Funk. Regulatable promoters of Saccharomyces cerevisiae: comparison of transcriptional activity and their use for heterologous expression. *Nucleic Acids Research*, 22(25):5767–5768, December 1994.

[47] Kevin F Murphy, Gabor Balazsi, and James J Collins. Combinatorial promoter design for engineering noisy gene expression. *Proceedings of the National Academy of Sciences of the United States of America*, 104(31):12726–12731, January 2007.

[48] Dmitry Nevozhay, Rhys M Adams, Kevin F Murphy, Kresimir Josic, and Gabor Balazsi. Negative autoregulation linearizes the dose-response and suppresses the heterogeneity of gene expression. *Proceedings of the National Academy of Sciences of the United States of America*, 106(13):5123–5128, March 2009.

[49] T L Orr-Weaver, J W Szostak, and R J Rothstein. Yeast transformation: a model system for the study of recombination. *Proceedings of the National Academy of Sciences of the United States of America*, 78(10):6354–6358, October 1981.

[50] M Papamichos-Chronakis, R S Conlan, N Gounalaki, T Copf, and D Tzamarias. Hrs1/Med3 is a Cyc8-Tup1 corepressor target in the RNA polymerase II holoenzyme. *Journal of Biological Chemistry*, 275(12):8397–8403, March 2000.

[51] Manolis Papamichos-Chronakis, Theodoros Petrakis, Eleni Ktistaki, Irini Topalidou, and Dimitris Tzamarias. Cti6, a PHD domain protein, bridges the Cyc8-Tup1 corepressor and the SAGA coactivator to overcome repression at GAL1. *Molecular Cell*, 9(6):1297–1305, June 2002.

[52] Basant K Patel, Jackie Gavin-Smyth, and Susan W Liebman. The yeast global transcriptional co-repressor protein Cyc8 can propagate as a prion. *Nature Cell Biology*, 11(3):344–349, February 2009.

[53] Hilary Phenix, Katy Morin, Cory Batenchuk, Jacob Parker, Vida Abedi, Liu Yang, Lioudmila Tepliakova, Theodore J Perkins, and Mads KAErn. Quantitative Epistasis Analysis and Pathway Inference from Genetic Interaction Data. *PLoS Computational Biology*, 7(5):e1002048, May 2011.

[54] Priscilla E M Purnick and Ron Weiss. The second wave of synthetic biology: from modules to systems. *Nature reviews Molecular cell biology*, 10(6):410–422, June 2009.

[55] Prasuna Ratna, Simone Scherrer, Christoph Fleischli, and Attila Becskei. Synergy of repression and silencing gradients along the chromosome. *Journal of molecular biology*, 387(4):826–839, April 2009.

[56] Nitzan Rosenfeld, Jonathan W Young, Uri Alon, Peter S Swain, and Michael B Elowitz. Gene regulation at the single-cell level. *Science (New York, NY)*, 307(5717):1962–1965, March 2005.

[57] R J Rothstein and F Sherman. Genes affecting the expression of cytochrome c in yeast: genetic mapping and genetic interactions. *Genetics*, 94(4):871–889, April 1980.

[58] R K Saiki, D H Gelfand, S Stoffel, S J Scharf, R Higuchi, G T Horn, K B Mullis, and H A Erlich. Primer-directed enzymatic amplification of DNA with a thermostable DNA polymerase. *Science (New York, NY)*, 239(4839):487–491, January 1988.

[59] Z Shao, H Zhao, and H Zhao. DNA assembler, an in vivo genetic method for rapid construction of biochemical pathways. *Nucleic Acids Research*, 37(2), January 2009.

[60] Sean C Sleight, Bryan A Bartley, Jane A Lieviant, and Herbert M Sauro. In-Fusion BioBrick assembly and re-engineering. *Nucleic Acids Research*, 38(8):2624–2636, May 2010.

[61] Stephen T Smale and James T Kadonaga. The RNA polymerase II core promoter. *Annual Review Of Biochemistry*, 72:449–479, January 2003.

[62] H O Smith and K W Wilcox. A restriction enzyme from Hemophilus influenzae. I. Purification and general properties. *Journal of molecular biology*, 51(2):379–391, July 1970.

[63] R L Smith and A D Johnson. Turning genes off by Ssn6-Tup1: a conserved system of transcriptional repression in eukaryotes. *Trends in Biochemical Sciences*, 25(7):325–330, July 2000.

[64] K Struhl. Fundamentally different logic of gene regulation in eukaryotes and prokaryotes. *Cell*, 98(1):1–4, July 1999.

[65] M A Treitel and M Carlson. Repression by SSN6-TUP1 is directed by MIG1, a repressor/activator protein. *Proceedings of the National Academy of Sciences of the United States of America*, 92(8):3132–3136, April 1995.

[66] S Ugolini and CV Bruschi. The red/white colony color assay in the yeast Saccharomyces cerevisiae: Epistatic growth advantage of white ade8-18, ade2 cells over red ade2 cells. *Current genetics*, 30(6):485–492, January 1996.

[67] Ernst Weber, Carola Engler, Ramona Gruetzner, Stefan Werner, and Sylvestre Marillonnet. A modular cloning system for standardized assembly of multigene constructs. *PloS one*, 6(2):e16765, 2011.

[68] F E Williams, U Varanasi, and R J Trumbly. The CYC8 and TUP1 proteins involved in glucose repression in Saccharomyces cerevisiae are associated in a protein complex. *Molecular And Cellular Biology*, 11(6):3307–3316, June 1991.

[69] K H Wong and K Struhl. The Cyc8-Tup1 complex inhibits transcription primarily by masking the activation domain of the recruiting protein. *Genes and Development*, 25(23):2525–2539, December 2011.

[70] Baogong Zhu, Guifang Cai, Emily O Hall, and Gordon J Freeman. In-fusion assembly: seamless engineering of multidomain fusion proteins, modular vectors, and mutations. Technical report, Dana-Farber Cancer Institute, Harvard Medical School, Boston, MA 02115, USA., September 2007.

Appendix: List of Reagents and Equipment

Item	**Source**
Primers	Invitrogen, Life Technologies
EcoRI	NEB Catalog# R3101L
XbaI	NEB Catalog# R0145L
SpeI	NEB Catalog# R0133L
PstI	NEB Catalog# R3140L
NEBuffer 2	NEB Catalog# B7002S
BSA	NEB Catalog# B9001S
Phusion	Phusion High-Fidelity DNA Polymerase (F-530)
5x HF buffer	Phusion HF Buffer Pack (F-518L)
dNTP	NEB Catalog# N0447L
Gel Extraction Kit	Bio Basic BS654-250Preps
PCR Purification Kit	Bio Basic BS664-250Preps
Plasmid DNA Kit	BS614-250Preps
Geniticin	G418, Wisent, Inc.
clonNAT	nourseothricin, Werner BioAgents, Jena

YPD	10 g/L yeast extract, 20 g/L bacteriological peptone (Wisent, Inc.), 2% (w/v) glucose (Sigma)
SC without uracil	6.7 g/L yeast nitrogen base without amino acids (Wisent, Inc.), 1.92 g/L yeast synthetic drop- out media supplement without uracil (Sigma), and 20 g/L agar (Wisent, Inc.), 2% (w/v) glucose (Sigma)
thermocycler	Eppendorf AG 22331 Hamburg
flow cytometer	Cyan-ADP 9 Beckman Coulter